Offshore Wind Turbine Access Using Knuckle Boom Cranes

Magnus Berthelsen Kjelland

Offshore Wind Turbine Access Using Knuckle Boom Cranes

Doctor of philosophy at the faculty of engineering and science,
specialisation in mechatronics

University of Agder

Faculty of Engineering and Science
2016

Doctoral Dissertation by the University of Agder 142
ISSN: 1504-9272

ISBN: 978-82-7117-836-9

Printed by: Wittusen & Jensen
Oslo

Preface

The work described in this thesis has been carried out at the University of Agder, Department of Engineering Sciences during the period 2011-2014. The work has been conducted under my principal supervisor Professor Michael Rygaard Hansen and co-supervisor Professor Geir Hovland, both from University of Agder.

Acknowledgements

First of all I would like to thank my principal supervisor Professor Michael Hansen for helping me in my research, even with a fully packed schedule. Working at night and in vacations don't seem to stop him helping me, finish my work. Also, a sincere thank you to Professor Geir Hovland for his guidance and help. During my work I was invited to visit STL Research in the U.K. I would like to thank Dr. David Kirkley for his hospitality during my visit. This project has been carried out in conjunction with Norwegian Centre for Offshore Wind Energy (NORCOWE). NORCOWE is an interdisciplinary resource centre for exploitation of offshore wind energy as a natural sustainable energy source. On a regular basis there have been meetings to discuss the project and once a year there has been a summer school, where a variety of different offshore wind related topics have been dealt with, together with visits to companies working in the offshore wind business. I would like to thank UIA, Geir Hovland (again) and NORCOWE for making the motion laboratory available for my research. It has been a privilege to work in these settings. Having a full scale vehicle loader crane and two Stewart platforms to "play" with is indeed a motivation. A great thanks to my fellow colleagues in my office, Ilya, Yulin, Øyvind and Knut. Our office has from day one been an environment for new ideas and support in my work. The lab personnel at the university have been very supportive and provided help to all the practical work needed in the installation of the motion lab and in my project. Many thanks to Eivind, Roy, Calle and Yousef. Finally, thanks for the support from my family and friends.

Abstract

There is a great need for renewable and sustainable energy today and there are several different sources for this energy where offshore wind is one that has a great estimated planned power production. Wind power production has for many years been produced onshore, but installing the wind turbines offshore has some benefits due to higher and more stable wind conditions. The majority of installed wind turbines are today bottom fixed, but when moving to deeper waters it is too high cost in building and installing foundation, which brings the possibility of using floating wind turbines. There are, however, also challenges due to the access for both the fixed and floating offshore wind turbines. During startup, repair or maintenance there is a demand for easy access of both personnel and equipment.

This dissertation mainly deals with offshore access solutions systems or parts of those systems. The access solutions are systems that transfers personnel or equipment from a floating vessel to a fixed or floating offshore structure.

Work done using a small scale hydraulic manipulator is described in Papers A and B, where paper A deals with the kinematic motion control of such a small scale redundant manipulator mounted on a moving Stewart platform, imitating the motion of a floating vessel. The manipulator tries to keep the tool point at a fixed reference point by the use of the pseudo-inverse Jacobian. Used in the experimental verification is a high precision laser tracker which measures the position of the tool point. Paper B uses the same manipulator and has in addition a hanging payload

attached to the tool point. A LQR control strategy is used to minimize the vibration of the hanging payload when the manipulator moves the tool point relative to a ground fixed coordinate system.

Paper C is concerned with the inherent oscillatory nature of pressure compensated motion control of a hydraulic cylinder subjected to a negative load and suspended by means of a counter-balance valve. The method proposed in this paper has the focus on pressure feedback and is compared to classical control strategies.

In paper D input shaping is used for the slewing motion control of a full scale mobile crane. The flexibility of the crane causes vibrations when slewing and by knowing the natural frequency and damping, the command signal is shaped so there are no residual vibrations. Experimental verification is carried out by means of a laser tracker.

Finally, the work done in Paper E deals with active heave compensation from a fixed structure to a floating vessel. Modeling of the hydraulic winch is done and a frequency response function is obtained. The active heave compensation was experimentally verified using the full scale mobile crane as the fixed structure with a winch mounted on it and the Stewart platform as the moving structure. Both results from active heave compensation and constant tension are presented. The payload in the experiments is a 400kg steel structure.

Publications

The following four papers are appended and will be referred to by their character. The papers are printed in their originally published state except for changes in format and minor errata.

A. M. Kjelland, I. Tyapin, G. Hovland and M. Hansen , "Tool-Point Control for a Redundant Heave Compensated Hydraulic Manipulator", *Proceedings of the 2012 IFAC Workshop on Automatic Control in Offshore Oil and Gas Production*,pages 299-304, doi:10.3182/20120531-2-NO-4020.00034, May 31 - June 1, 2012.

B. M. Kjelland, I. Tyapin, G. Hovland and M. Hansen, "Tool-Point Control of a Planar Hydraulically Actuated Manipulator with Compensation of Non-Actuated Degree of Freedom", *Control, Automation and Systems (ICCAS), 2012* 12^{th} *International Conference on*, pages 672-677, 2012.

C. M. Kjelland and M. Hansen, "Numerical and Experiential Study of Motion Control Using Pressure Feedback", *The* 13^{th} *Scandinavian International Conference on Fluid Power, SICFP2013*, June 3-5, 2013.

D. M. Kjelland and M. Hansen, "Offshore Wind Payload Transfer Using Flexible Mobile Crane", *Journal of Modeling, Identification and Control, MIC*, .

The following papers have been submitted and is considered a part of the thesis..

E. M. Kjelland and M. Hansen, ”Using Input Shaping and Pressure Feedback to Suppress Oscillations in Slewing Motion of Lightweight Flexible Hydraulic Crane”, *Submitted to: Journal on Fluid Power*, .

The following paper is not included in the dissertation but constitute an important part of the background and is reffert to in the introduction.

F. M. Kjelland and M. Hansen, ”Tool point tracking for redundant hydraulic actuated manipulator using velocity control”, 7^{th} *FPNI PhD SYMPOSIUM on FLUID POWER*, June 27-30, 2012.

Contents

List of Figures

Chapter 1

Introduction

1.1 Motivation and Problem Statement

Windmills have been in use for many centuries. They were used for mechanical labour, such as grinding grains or pumping water. Wind turbines on the other hand are machines that converts kinetic energy in the wind to electrical power. The modern wind power industry did not start until the late 1970s, and from this point the research within wind power has accelerated.

Wind energy is one of the most promising sources for renewable energy. According to The World Wind Energy Association the worldwide capacity at the end of 2012, has reached 282.275 [MW] and 318.529 [MW] by end of 2013. Since 2001, the annual growth in capacity has been about 21%, however the last year only experienced a 12.7% growth. The top world leading countries are China, USA, Germany, Spain and India.
The majority of the installed capacity is on land. In the latest years some offshore parks have been built. Some of the major offshore wind farms in Europe are located in the UK and Denmark. Greater Gabbard (UK), Whalney (UK), Sheringham Shoal (UK), Horns Rev (DK) and Rødsand (DK) and Dogger Bank (UK) are some examples on newly developed offshore wind farms, see (Bakka, 2013). The turbines in these farms are installed in shallow waters, where the turbines are either fixed to the soil or they stand on monopoles or other structures.

For countries such as Spain, US, Japan, Korea, Scotland and Norway it would be beneficial to also be able to install wind turbines in deeper waters, in depths up to several hundred meters. The existing well established bottom fixed turbines are not suited for such deep water. During the last couple of years floating solutions have started to emerge. Hywind is one example of a floating wind turbine solution, see (EWEA, 2013). The demonstration turbine was installed back in 2009 and is still in operation. It is located in the North Sea, right off the Norwegian west coast.

1.1.1 Background

Today the cost of operating, maintaining and repairing offshore wind turbines are high. To make offshore wind power more attractive, this cost must be lowered. One way to do this is to lower the cost of transporting people and equipment to the offshore wind turbines. This can be done through new and innovative technology.
With all the new developments on bottom fixed and floating wind turbines, there also appears a need for maintenance and repair. The wind turbines may easily be located 100 km from shore and access is both weather dependent and expensive. Even if a wind turbine does not break down, it still requires maintenance and inspection of components. This means that maintenance and repair personnel must visit every wind turbine in a certain interval. There is a great economical potential in having a good and robust access solution for the offshore wind turbine, whether it has a fixed or floating foundation.
One of the main difficulties with access to the wind turbines are the disturbance from the the weather and, predominantly, the ocean waves. In order to access an offshore wind turbine a certain weather window is required. Hence, a weather window is simply some tolerances on wind and waves that allow for safe operations. Increasing this weather window is highly important for offshore wind since it reduces the risk and uncertainty associated with offshore access.
Vessel to vessel or vessel to fixed structure transportation of personnel and equipment can be achieved by compensation of the payload in reference to the landing point, whether it is a moving or a fixed point. In this work the payload transfer is to be carried out between a vessel and a fixed or floating wind turbine installation.

In order to achieve this, some kind of topology is required, that involves the vessel with a dynamic positioning system, the wind turbine installation (either fixed or floating), the load transferring unit, and one or more motion sensors, see Figure 1.1. In total, this will be referred to as a Payload Access and Transfer Solution (PATS).

Figure 1.1: *Example of an Offshore Access solution for payload transfer. Photo courtesy of Maersk.*

There exist many PATS in the current offshore market. However, it is expected that there will be a demand for lifting payloads with masses around 1..2 metric tonnes when installing and servicing offshore wind turbines. This type of load is significantly larger than personnel carriers and significantly smaller than heavy duty lifting.

1.1.2 Current Payload Access and Transfer Solutions (PATS)

Today, there are several solutions for accessing an offshore wind turbine, see Figure 1.2. There exists a wide variety of solutions, however, the ones shown in Figure 1.2 represent those most relevant for the payload sizes envisaged in the current project. Ampelmann, (Ampelmann, 2015), a Dutch based company uses a hydraulically actuated hexapod or Stewart platform to compensate for the movements created by the ocean.

Figure 1.2: *Example of existing offshore PATS. Top left is Ampelmann, top right is Maxcess, bottom left is Uptime, and bottom right is Palfinger.*

On top of the hexapod is a gangway where the personnel can simply walk from the vessel to the wind turbine. Palfinger is another company that offers a crane winch to transfer payload from a vessel to the base or to the top of the wind turbine, see (Palfinger, 2015). Maxcess, (Power, 2015), has developed a mechanical access platform located at the bow of a small vessel that attaches to the wind turbine structure. By hanging passively onto the wind turbine the personnel can climb up and down from the wind turbine. Finally, Uptime, (Uptime, 2015), has created a motion compensated bridge that can transport personnel.

1.1.3 Research Question

When examining the access solutions they can be categorized based on their mechanical structure, degrees of freedom (DOF), type of actuation, or type of vessel-structural contact. The Ampelmann solution is a combination of a six DOF closed chain mechanism with a three DOF open chain bridge on top. This gives a total of nine DOF's allowing for a full spatial motion compensation with a degree of redundancy (DOR) of three. The Uptime bridge corresponds to the Ampelmann bridge, i.e., three DOF which only allows for positional heave compensation without the

ability to compensate for orientation offset, and the Palfinger solutions has only a single active DOF in the winch which reduces the compensation to purely vertical heave compensation. Finally, the Maxcess locks the vessel to the wind turbine structure by means of thrust and friction. This corresponds to forced point contact. If the solutions are compared, it is obvious that they have different advantages and disadvantages. In general, the Maxcess solution has the most limited weather window and also the lowest possible payload transfer. The solution will always subject the wind turbine installation to a high structural load during access. On the other hand, it is a safe and simple connection that does not require any active compensation. The Palfinger solution is limited to hanging payloads but is otherwise well suited because of the inherent advantages of knuckle boom cranes: small footprint, low weight, low price. The active compensation only needs to be applied to a single DOF (the winch motor). The Uptime solution allows for a full position compensation but it needs to handle different types of motion: slew, boom, and telescopic. Both boom and telescopic motion are more prone to friction and non-linearities and therefore constitute a more complex control challenge. Finally, the Ampelmann is easily the most complex but also the only solution that allows for a full compensation. Except for the Palfinger solution, none of the solutions are prepared to handle any type of weight lifting and the Palfinger solution is used as inspiration for the main theme of this work. In fact, Palfinger is the largest supplier of vehicle loader cranes. Commercial vehicle loader cranes are weight optimized hydraulically actuated knuckle boom cranes with a low eigenfrequency as compared to an offshore knuckle boom crane. The advantages mentioned for the Palfinger offshore crane are even more pronounced if a vehicle loader crane was introduced. In addition, they are very well suited for payload masses in the range 1 to 2 metric tonnes, i.e., significantly above transport of personnel and significantly below heavy duty lifting. The big challenge is to do the motion compensation with such a hydraulic manipulator since this has never been done before.

Therefore the main research question of this project is twofold: to identify and put forward solutions to the main challenges associated with employing hydraulically actuated manipulators in the shape of vehicle loader knuckle boom cranes for the

transfer of payload from vessel to vessel subjected to wave induced motion disturbances. There are a number of unresolved motion compensation issues related to this topic encompassing tool point control of:

- redundant actuated manipulators
- manipulators with free hanging payload
- flexible manipulators

All of these issues must be handled taking into account the hydraulic actuation that is characterized by phenomena such as saturation, nonlinearity and oscillatory behavior. The purpose of this project has been to explore these issues both theoretically and experimentally during the project period and publish the findings in a number of scientific papers as well as the thesis.

1.2 State of the Art

Payload transfer using a vehicle loader crane corresponds to working on closed loop motion control of an open chain mechanism with emphasis on the tool point behavior. The fundamental building blocks to be considered in such a system are: motion sensors, disturbances, control strategy, and mechanical system.

In general, a full 3D motion compensation is to measure the position and orientation of the target platform relative to the source platform, as well as the time derivatives of the relative motion. These values may be used as reference motion input to a controller driving the payload manipulator on the source platform.

The motion sensors must give the absolute motion of any non-fixed vessel involved in the payload transfer. In Figure 1.3 the coordinate system used represents the vessels centre of gravity and is defined as:

$$\vec{R}_V = \begin{bmatrix} X_V \\ Y_V \\ Z_V \end{bmatrix} \tag{1.1}$$

The orientation of the vessel in reference to the fixed world coordinate is, in general, given by three independent angles: θ_x, θ_y and θ_z, but normally a more operational way of representing these angles is via a 3 by 3 transformation matrix.

$$\mathbf{A}_V = \mathbf{A}_V(\theta_x, \theta_y, \theta_z) \tag{1.2}$$

The transformation matrix transforms coordinates from a global world coordinate system, X, Y and Z in Figure 1.3, to that of the vessel($\xi\ \eta\ \zeta$).
Let

$$\vec{S'}_{(V\to P)} = \begin{bmatrix} \xi_{(V\to P)} \\ \eta_{(V\to P)} \\ \zeta_{(V\to P)} \end{bmatrix} \tag{1.3}$$

and

$$\vec{S}_{(V\to P)} = \begin{bmatrix} X_{(V\to P)} \\ Y_{(V\to P)} \\ Z_{(V\to P)} \end{bmatrix} \tag{1.4}$$

be the same vector for V to any point P measured in earth (X,Y,Z). In that case

$$\vec{S}_{(V\to P)} = \mathbf{A}\vec{S'}_{(V\to P)} \tag{1.5}$$

$$\vec{S'}_{(V\to P)} = \mathbf{A}^{-1}\vec{S}_{(V\to P)} \tag{1.6}$$

There are different ways to estimate the motion of a moving vessel. Various sensing elements and technology are used in each sensor. Some of them are: Motion Reference Unit (MRU), Global Position System (GPS), Radio Sounders, Laser Tracking, Vision and Echo sounding or Sonar.

In this thesis the focus will be on systems using the motion reference unit (MRU). This type of sensor uses both a three axis accelerometer and a three axis gyroscope to measure the the absolute position of some point, M, on the vessel, see

Figure 1.3, as well as the three orientation angles.

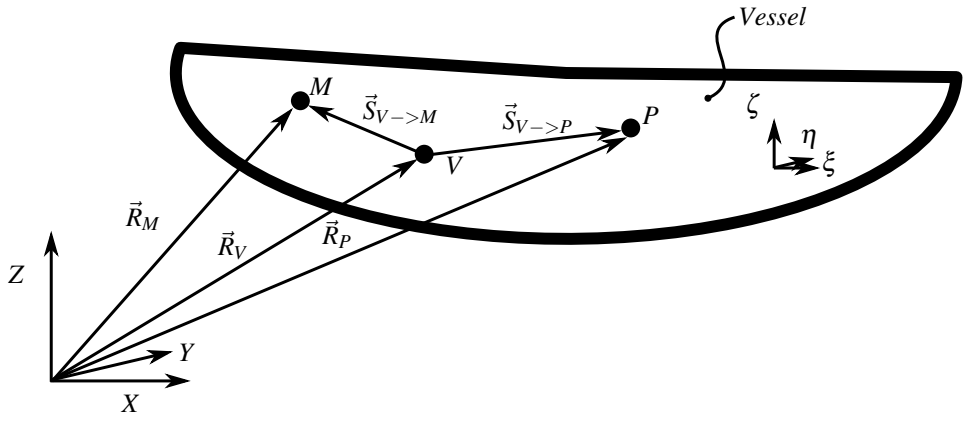

Figure 1.3: *Coordinate system*

This way, it is always possible to find the position of the mass centre, V, and any other point of interest, P, using Eqs. (1.7) - (1.9). Similarly, velocities and accelerations of any point P can be estimated based on the measurements of velocity and acceleration of M as well as the angular velocity and angular acceleration of the vessel.

$$\vec{R}_V = \vec{R}_M - \vec{S}_{(V\to M)} = \vec{R}_M - \mathbf{A}_V^T \cdot \vec{S}'_{(V\to M)} \tag{1.7}$$

$$\vec{R}_P = \vec{R}_M - \vec{S}_{(V\to M)} + \vec{S}_{(V\to P)} = \vec{R}_V + \vec{S}_{(V\to P)} = \vec{R}_V + \mathbf{A}_V^T \cdot \vec{S}'_{(V\to P)} \tag{1.8}$$

$$\dot{\vec{R}}_P = \dot{\vec{R}}_V + \vec{\omega}_V \times \mathbf{A}_V^T \cdot \vec{S}'_{(V\to P)} \tag{1.9}$$

1.2.1 Wave Disturbance

In order to evaluate and test methods for heave compensation it is necessary to model the disturbances from the waves.

The wave disturbance represented by a Modified Pierson-Moskovitz spectrum

is used in both simulations and experiments in the current work. It is written as:

$$\mathbf{S}_{\zeta\zeta}(\omega) = \frac{A}{\omega^5} e^{\frac{-B}{\omega^4}} \tag{1.10}$$

$$A = \frac{172.53 H_{1/3}^2}{\overline{T}^4} \tag{1.11}$$

$$B = \frac{689.97}{\overline{T}^4} \tag{1.12}$$

where $H_{1/3}$ is the significant wave height and $\overline{T}$ is the average wave period. Simulation of the sea surface elevation is described in work by (Perez, 2005) and defined by:

$$\zeta(t) = \sum_{n=1}^{N} \sqrt{2\mathbf{S}_{\zeta\zeta} \cdot \omega_n^* \cdot \Delta\omega} \cdot \cos(\omega_n^* t + \varepsilon_n) \tag{1.13}$$

$$\omega_n^* = w_n \in [\omega_n - \frac{\Delta\omega}{2}, \omega_n + \frac{\Delta\omega}{2}] \tag{1.14}$$

where N is the number of wave frequencies, ω_n is chosen by fixed steps of $\Delta\omega$ that is the step between two adjusted frequencies $(\omega_{(n+1)} - \omega_n)$, ω_n^* is the n-th frequency and is chosen randomly in its domain defined in (1.14), t is time and $\varepsilon_n \in [0, 2\pi]$ is the phase that is chosen randomly for each wave frequency.
Using (1.13), a time series of the sea surface elevation or heave motion can be created.

The sea surface elevation can be used to calculate the motion of the vessel by using the vessels response amplitude operator (ROA). This is a set of transfer functions which can be obtained using commercial software or by experimentation. The transfer function contains the amplification and phase shift for each degree of freedom of the vessel and they depend on the angle of the vessel in reference to the incoming waves.

With a suitable set of MRUs it is possible to know both source and target frame for an offshore payload transfer, and thereby converting the task into a a tool point

control of the manipulator. In that case any payload transfer can be reduced to a tool point control task with the purpose of minimizing the deviation of the position and/or velocity of the tool point relative to reference values. The tool point can be a hook that a hanging load is attached to, or it can be a gripper tool that fixates an object but quite often the payload will be connected to the tool point of the manipulator as a pendulum via a non-actuated kinematic joint. This type of tool point control is often referred to as coordinated control if the manipulator has several degrees of freedom or heave compensation if it is an offshore application. In this thesis the term tool point control will be preferred.

1.2.2 Tool Point Control

Tool point control for a non-redundant manipulator is based on reference motion obtained from inverse kinematics and a reference tool point. Inverse kinematic control for hydraulically or electrically actuated machines has been done by (Cinkelj et al., 2010) and (Kucuk and Bingul, 2004). Non-redundancy simplifies the inverse kinematics, however, it minimizes the possibility of influencing the reference motion. Tool point control by redundant manipulators has been investigated by (Beiner and Mattila, 1999) and (Park et al., 2001). Unlike non-redundant manipulators a scheme is required for choosing among the infinite number of actuator velocities that will yield the desired motion, however, this automatically introduced the possibility of optimizing the reference motion, typically by controlling the null space motion of the manipulator. Work has been done to find optimization functions that can increase performance by controlling the null space motion. An approach by (Han and Chung, 2007) has been minimization of restoring moments and redundancy must be taken into account in this thesis since the vehicle loader crane inherently has one degree of freedom actuation redundancy. For hanging loads the main objective of the heave compensation is to control the velocity of the payload mass center relative to either an inertial or moving frame depending on the nature of the source and target of the payload transfer. The main challenge is, of course, that the payload is suspended by an unactuated joint. This corresponds to stabilizing a pendulum, see for example (Wen et al., 1999) and (Chunhacha and Benjanarasuth, 2011). Hanging loads are common place within offshore payload transfer, hence, this is also a

topic that must be considered in this work. The cranes to be investigated in this thesis are all hydraulically actuated. This introduces a number of control challenges due to saturation phenomena, non-linearities and stability problems when handling negative loads. The use of overcenter valves or counterbalance valves are widely used in hydraulics on such applications as cranes, telehandlers and winches as an integrated part of the actuator control. They are distributed to each actuator (degree of freedom) depending on the type of external loading. They a multi-functional and, normally, they serve at least the following functions:

- leak tight load holding
- shock absorption
- cavitation protection at load lowering
- load holding at pipe burst
- no drop before lift

It is, however, well known that they tend to introduce instability in a system, especially when the flow supply is pressure compensated. Since this combination is a de-facto standard in a wide range of machinery this poses a major challenge to the present day hydraulic systems designer. This problem has attracted a lot of attention with emphasis on modeling and parameter variation (Miyakawa, 1978), (Overdiek, 1980), (Overdiek, 1981), (T Persson and Palmberg, 1989) and (Nordhammer et al., 2012) revealing a number of common stabilizing characteristics. They include increased volume between directional valve and actuator, reduced pilot area ratio as well as reduced gravitational and inertia load, whereas the influence by a number of other design variables remain less obvious, see also (H Handroos and Vilenius, 1993). Stability is only one of several performance parameters for an overcenter valve system and therefore, as pointed out in in (Chapple and Tilley, 1994) choosing/designing an overcenter valve for a specific application is complicated. The widespread use of the pressure compensation is mainly due to two basic functionalities

- it allows several actuators to be driven simultaneously with minimal influence between the different active circuits.

- the valve flow and thereby the actuator speed is a well-defined function of the control signal removing the disturbing influence from fluctuating loads.

Therefore, we must address the challenge of suppressing the oscillatory nature of an overcenter valve system taking into account that the above mentioned design criteria cannot be ignored. In (P A Nordhammer and Hansen, 2012) an alternative approach that simply moves the main throttling from the overcenter valve to the return orifice of the main directional control valve is introduced. That gives a stable system, however, the acceptable load variation is quite limited. In (Hansen and Andersen, 2010) a pressure feedback scheme that has as target to maintain the high pass filtered pressure gradient equal to zero is described. It gives a stable system, however, it requires valve bandwidth that lies in the high-end of what is obtainable with proportional valves typically used in vehicle loader cranes. Even though instability can be avoided then the use of weight optimized loader cranes means that the task of controlling a long flexible mechanical structure. Hence, vibrations and deflections that are detrimental to efficient and safe operations may occur even with a stable or well designed actuation system. Work regarding control of vehicle loader crane often includes tool point control (Ebbesen et al., 2006) and (Pedersen et al., 2010) where the flexibility is included and clearly indicate that the performance of tool point control is influenced by structural vibrations caused in the crane. Some efforts to reduce this effect can be seen in (Hansen and Andersen, 2010). A successful approach to reducing unwanted dynamics in machinery with low damping and low eigenfrequencies is called input shaping. Input shaping is an open loop control technique used to filter reference commands in such a way that they cancel out their own motion induced oscillations (Sorensen et al., 2010). Input shaping is particularly effective for lightly damped oscillations in low frequency systems, such as overhead cranes with the payload suspended by wires (Singhose and Seering, 2011). There are no example of applying the method to hydraulically actuated boom cranes, although, recently (Moon, 2012) used input shaping on a pneumatically actuated and downscaled excavator arm. In the offshore environment any type of motion control that compensates for wave induced motion is normally referred to as heave compensation. The payload transfer investigated in this project is, basically, a heave compensation task as seen from an offshore point of view. No work has been reported on

heave compensation using boom control on vehicle loader cranes or other knuckle boom cranes, however, similar work regarding modeling and control of a hydraulic winches have been done by several researchers. (Than et al., 2002), investigated constant tension and heave compensation in a purely simulated environment. Work by (Neupert et al., 2008) also propose a prediction method to increase performance of heave compensation. Standard industrial crane control concerning active heave compensation and constant tension has been used for many years, especially in the oil and gas industry, see (NSO, 2013). An approach to damping the payload in active heave compensation has successfully been done in simulation by (Yuan, 2010). Work done by (Johansen et al., 2003) show experimental results of an active heave compensation system. The paper focuses on wave synchronization when lowering a payload in a moonpool environment. A detailed modeling of a hydraulic active heave compensated system can be found in (Sverdrup-Thygeson, 2007). In critical subsea operations, such as landing payloads on the seabed, there is a dependency on active heave compensation. Work with a focus on rope dynamics has been carried out by (Imanishi et al., 2009) where the application is on a hydraulic winch, but without any heave compensation. Predictive control of a hydraulic winch has been done in simulation by (Entao et al., 2009), where real-time parameter estimation is used to improve the motion control of the winch. Work regarding another control approach such a feed-forward control has been done by (Entao and Wenlin, 2009). In (Haaø et al., 2012) the focus is on the friction on a heave compensation system, however the system is different from the hydraulic winch. Work regarding constant tension on a hydraulic winch is described by (Engedal and Egelid, 2011).

1.3 Outline

Part I contains a chapter on the modeling and simulation of the vehicle loader crane as a hydraulically actuated mechanical system. Part I also contains a chapter on the different types of control strategies that have been developed with a view to introduce different types of heave compensation needed in a PATS. Part II consists of a collection of edited papers. This part consists of a collection of five contributed papers denoted paper A ... E, introduced below. Summary and background of each

paper are given. The last section includes the overall contributions of the work presented in the thesis.

Paper A: Tool-Point Control for a Redundant Heave Compensated Hydraulic Manipulator

Summary: In this paper, theoretical and experimental implementation of heave compensation on a redundant hydraulically actuated manipulator with 3-dof has been carried out. The redundancy is solved using the pseudo-inverse Jacobian method. Techniques for minimizing velocities and avoiding mechanical joint saturations is implemented in the null space joint motion. Model based feed-forward, combined with a PI-controller handles the velocity control of each joint. A dynamical model is created in multi body dynamic where the controller is implemented and tested. A time domain simulation model has been developed, experimentally verified, and used for controller parameter tuning. Model verification and experimental results are obtained while the manipulator is exposed to wave disturbances created in a dry environment by means of a Stewart platform.

Background and contribution: To verify the inverse kinematic control on a redundant hydraulic manipulator used for heave compensation on a moving platform. Validated by measuring the position for the tool point with a laser tracker.

Paper B: Tool-Point Control of a Planar Hydraulically Actuated Manipulator with Compensation of Non-Actuated Degree of Freedom

Summary: The current work is on motion control of a hydraulically actuated manipulator with a view to handle offshore payload transfer between moving frames. The manipulator has redundant actuation and also, a non-actuated degree of freedom. The motion control has two targets: tool point control and compensation

of the non-actuated degree of freedom. The redundancy is handled by means of pseudo-inverse kinematics while optimizing a cost function, avoiding mechanical joint limits. The compensation of the un-actuated degree of freedom employs LQR control, minimizing position and velocity error while maintaining the tracking reference for the tool-point. The proposed control scheme is implemented and experimentally validated in a practical system where the manipulator is mounted on a Stewart platform that allows for the simulation of wave induced heave motion as a disturbance.

Background and contribution: Development and experimental verification of vibration reducing control of non-actuated degree attached to the tool point of a hydraulic manipulator. Can be applied to a hanging payload.

Paper C: Numerical and Experiential Study of Motion Control Using Pressure Feedback

Summary: This paper is concerned with the inherent oscillatory nature of pressure compensated motion control of a hydraulic cylinder subjected to a negative load and suspended by means of an overcenter valve. A pressure feedback scheme that indirectly eliminates the oscillations is investigated. The indirect control scheme utilizes pressure feedback to electronically compensate the metering-out allowing for the removal of the compensator and, subsequently, elimination of the oscillations. The suggested electronic compensation scheme is implemented and examined in a single degree-of-freedom test rig actuated by means of a double acting hydraulic cylinder. The control scheme is compared with other control schemes and the importance of measurement filtering and controller cycle time are investigated.

Background and contribution: Comparison and evaluation of control strategies for controlling a hydro-mechanical system experiencing a negative payload. Mainly focus is on using pressure feedback in the control. Vibration reduction is

achieved, shown in the results.

Paper D: Using Input Shaping and Pressure Feedback to Suppress Oscillations in Slewing Motion of Lightweight Flexible Hydraulic Crane

Summary: This paper presents a method to actively reduce vibrations in the flexible mechanical structure of a hydraulically actuated vehicle loader crane. Based on information on the natural frequency and damping of a simplified model of the crane an input shaping scheme is set up to control the proportional valve leading to substantially reductions in oscillations. The method is compared and combined with a pressure feedback control of the proportional valve that actively suppresses variations in pressure. A full scale vehicle loader crane is used in the experimental verification of the method, and the motion of the tool point of the crane is measured by a high precision laser tracker. The results shown in this paper demonstrate that input shaping and pressure feedback are useful tools to minimize vibrations in hydraulically actuated flexible structures.

Background and contribution: Vibration can be a problem when controlling flexible structures. Input shaping control is applied which reduced the residual vibrations under and after the motion is performed.

Paper E: Offshore Wind Payload Transfer Using Flexible Mobile Crane

Summary: This article presents an offshore-simulated loading and unloading of a payload from a floating platform to a fixed structure. The experiments are performed in a dry-lab, where a Stewart platform is used to simulate the motion of the vessel. A hydraulically actuated vehicle loader crane is used to perform the tasks

of payload transfer. The crane includes a hydraulic winch where the wire force is measured by a load cell. A mathematical model of the winch is derived and is experimentally verified. The control strategies include a heave compensation and a constant tension mode. A motion reference unit is used to generate the reference motion of the moving platform. Experimental results show the wire force while performing the load cases. This paper shows the advantage of using a reference motion as a feed forward control reference, instead of only relying on the constant tension.

Background and contribution: Active heave compensation is used worldwide in applications as landing payload at sea-bottom from a floating vessel. Work in this article mainly focus on lifting and landing a payload from a fixed to a moving platform. Experimental evaluation of concept is presented.

1.4 Contributions

Working on the main scientific research question has led to a number of scientific contributions from this PhD project:

- Development and experimental implementation of active heave compensation in redundant hydraulically actuated manipulator.
- Development and experimental implementation of active heave compensation in redundant hydraulically actuated manipulator with hanging load (non-controlled DOF).
- Development and experimental implementation of boom motion using non-pressure-compensated mobile directional control valve.
- Development and experimental implementation of slew motion using a pressure-compensated mobile directional control valve.

- Development and experimental implementation of active heave compensation and active tension control using a winch and exploiting the structural flexibility of the tool point.
- The experimental identification for dynamic model the hydraulic winch, described in Papers E.
- The experimental evaluation of system for lifting and landing a payload while heave compensation on a moving Stewart platform, as described in Paper E.
- Development and experimental verification of vibration reduction while controlling flexible hydraulic crane using input shaping, shown in Paper D.
- Evaluation of control strategies for motion control of oscillatory system containing negative load and counterbalance valves.

Chapter 2

Hydraulic Manipulators

Machines using hydraulics as actuation are widely used in industry. Some machinery is quite compact, like hydrostatic transmissions or locking and clamping devices, other machinery is more slender and can be thought of as an articulated hydraulically arm. The latter is referred to as a manipulator in this context. Manipulators are, typically, found in:

- Mobile cranes or vehicle loader cranes
- Entrepreneur machinery
- Excavators
- Hydraulic robotics
- Deck Cranes or pipe handling cranes typical found in the oil industry
- Agricultural and forestry machinery

Normally, these types of machines has a human operator, controlling the manipulators using joysticks and their vision to observe how the machine is responding. Sensors are often used for safety measures, e.g. in interlocks. In some areas, such as the offshore oil industry, where equipment generally feature a high degree of automation closed loop motion or force control is more common as compared to other application areas.

Figure 2.1: *Hydraulic manipulators: Hydraulic robot (1) - Forestry machine (2) - Excavator (3) - Mobile crane (4) - Deck crane (5). (Photo courtesy of KNR System, Agrodetale, Deere, Rolls-Royce and Effer)*

The hydraulic manipulators may be treated as a multi-domain system consisting of three separate systems:

1. **Mechanical system:** This is the main load carrying physical structure. Often welded or bolted metal parts, containing the joints and the bodies of the manipulator.

2. **Electro-hydraulic actuation system:** This contains control valves, load holding / counter balance valves, cylinders and motors.

3. **Electronic control system:** This system consists of either a manual joystick or programmable logic controller (PLC). Based on the desired reference and response the operator or PLC controls the opening of the controls valves, thus the motion of the manipulator.

The actuation system on the manipulator consists of several hydraulic circuits supplied by a hydraulic power unit (HPU). The HPU deliver oil flow at a desired pressure (P_{supply}). The oil is consumed in the actuation system where it is turned into mechanical energy. Then the oil is returned to the HPU (T_{return}) for cooling and air bubble removal.

A simplified schematic of a typical motion control sub-system is shown in Figure 2.2. This circuit is controlling one degree of freedom (DOF) of the manipulator.

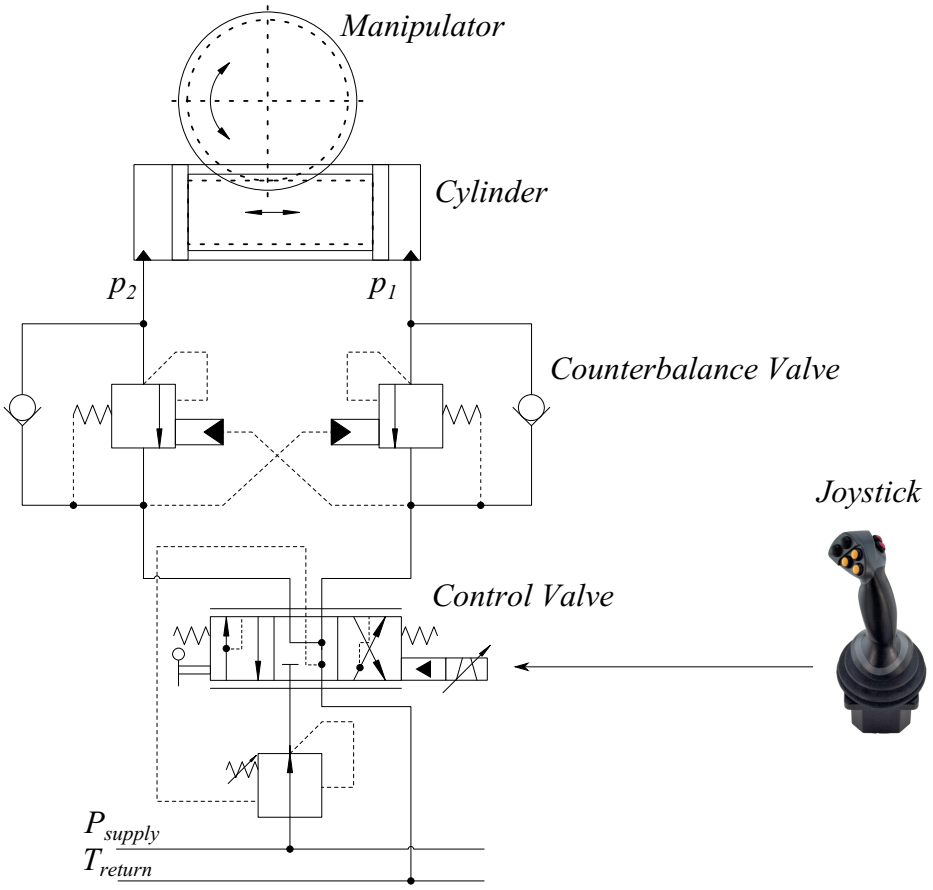

Figure 2.2: *Simple hydraulic system)*

The illustrated circuit is used to control the slewing of a manipulator and consists of a cylinder, a counterbalance valve (CBV) and a directional control valve (DCV) as the main components of the actuation system. The pressures in the cylinder chambers are p_1 and p_2. The motion of the cylinder is controlled by the opening of the DCV. The CBV will handle the situation if the cylinder experience a negative load (piston velocity and load force has the same direction), something that potentially can lead to simultaneous cavitation and pressure peaks in the cylinder chambers.
In many hydraulic manipulator application the DCV is pressure compensated. The reason for this is that it provides load independent flow control. This results in the

flow going through the DCV is proportional to the input signal, regardless of the load the system experiences.

In general, there are three main or typical hydraulically actuated degrees of freedom. They are boom motion (linear actuator), winch motion (rotational actuator), and swing motion (rotational actuator), see table 2.1.

Table 2.1: Manipulator Actuation

Actuation	Type	Dominant Effect
Swing	Rotational	Inertia
Boom	Linear	Gravity
Winch	Rotational	Gravity

In order to investigate all of these dominant degrees of freedom different test equipment has been used in this project. They can all be considered as different types of cranes with different topology, size, and dynamic characteristics.
A small hydraulic manipulator with a redundant configuration was used in development of tool point control for heave compensation control. It consists of one main boom and one knuckle boom, where the knuckle boom has a telescopic link, see Figure 2.3.

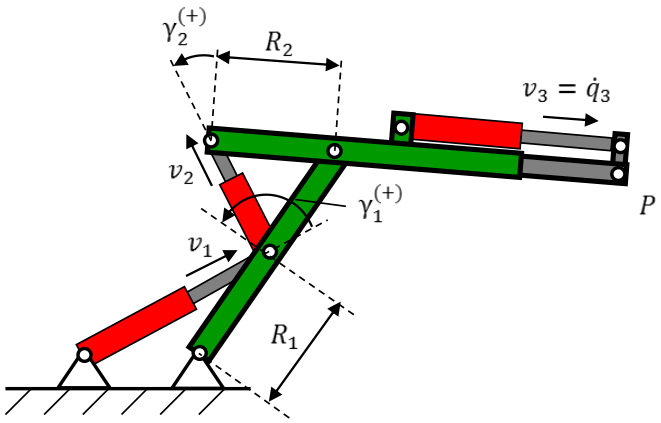

Figure 2.3: *Small hydraulic manipulator*

To evaluate and develop control for boom motion, a single degree of freedom hydraulic manipulator was used, see Figure 2.4. This manipulator was used to evaluate the vibration caused by the combined use of a pressure compensated DCV and a CBV when lowering the boom. The payload attached to the manipulator could be changed as well as the DCV and CBV.

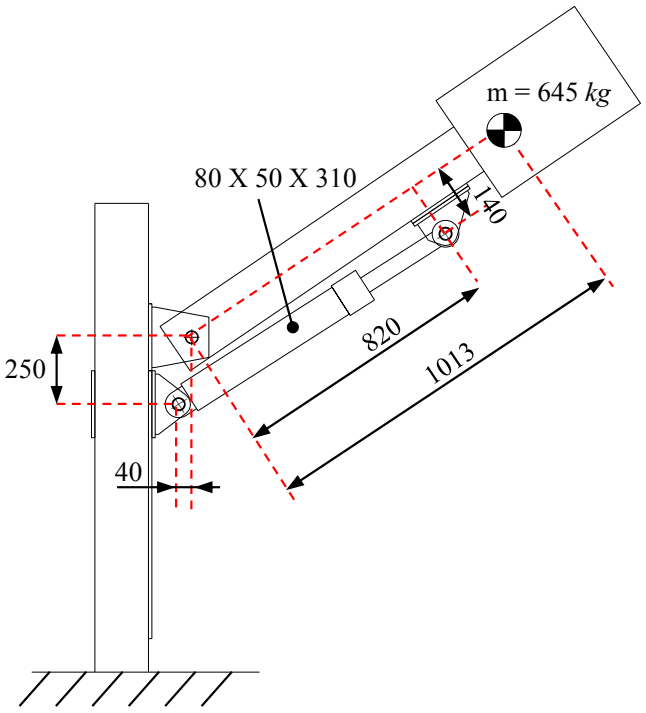

Figure 2.4: *Single boom manipulator*

The manipulator itself was mechanically designed ,so that the lower connection point for the cylinder could be moved down vertically in order to change the mechanical properties of the structure. The cylinder stroke was measured by a sensor.

The vehicle loader crane, a light-weight flexible manipulator, was used to develop tool point control with a large telescopic joint. The crane incorporates a slew axis which was used for the development of swing motion with reduced tool point vibration. A winch mounted on the crane was also used for heave compensation purposes.

By using the vehicle loader crane, experiments in a relevant industrial situation

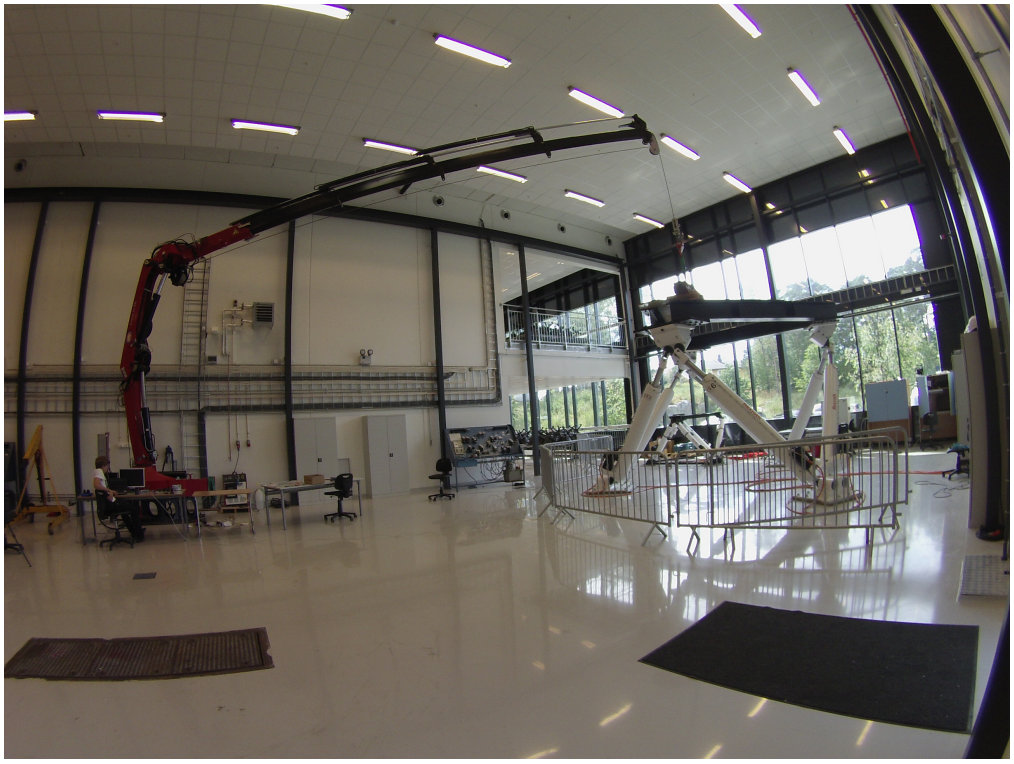

Figure 2.5: *Vehicle Loader Crane*

was evaluated.

As demonstrated in this chapter, there are many applications for hydraulic manipulators. The brief description of the different manipulators and their components used in this thesis gives an impression of the experimental work that was done.

Chapter 3

Modeling of Hydraulic Manipulators

The current thesis deals with motion control of hydraulic manipulators with emphasis on model based approaches in different ways. Hence, emphasis has not been on full-scale simulation models but more on using either rigid body kinematics, rigid body dynamics, hydraulic component characteristics and overall system dynamics in the development of control strategies. Therefore, the following chapter describes a number of modeling techniques associated with hydraulic manipulators and, more specifically, the test cranes listed in the previous section.

3.1 Kinematics

A kinematic model describes the motion of bodies without concern of the cause of the motion, such as forces and torques. It describes the relation between the position, velocity and acceleration of any mechanical systems. In rigid body kinematics these positions, velocities, and accelerations are limited to a fixed number of variables (3 in planar systems and 6 in spatial systems) for each body. Description on manipulator kinematics can be found in (Siciliano et al., 2010; Spong et al., 2006).

3.1.1 Position Kinematics

When setting up a kinematic model of a hydraulic manipulator it is possible to use the same techniques known from robotics and multibody dynamics. In positional analysis a correlation between the tool point frame and the joints of the manipulator

are of interest. The tool point frame coordinates and orientation (referred to as task space in robotics) represents the motion of the payload whereas the joint motion (referred to as joint space in robotics) represents the degree of freedom associated with the individual joints and thereby, directly or indirectly (depending on the way the actuator is connected to the mechanical system) the hydraulic actuators. Joint degrees of freedom can be purely rotational as in a revolute joint, or purely translational as in a prismatic joint or a combination as in a cylindrical joint. A crane often uses either a wire or a hook at its tool point, so the tool point frame orientation is of less importance as compared to robotics.

3.1.2 Forward Kinematics

The position $\mathbf{p}$ of the cranes tool point with reference to the base, given by the joint angles are found using the forward kinematics.

$$\mathbf{p} = f(\mathbf{q}) \tag{3.1}$$

where the vector $\mathbf{q} \in \mathbb{R}^n$ is the joint position, containing all the joint coordinates. The vector $\mathbf{p} \in \mathbb{R}^m$ are the absolute Cartesian coordinates, see Figure 3.1, of the cranes tool point frame.

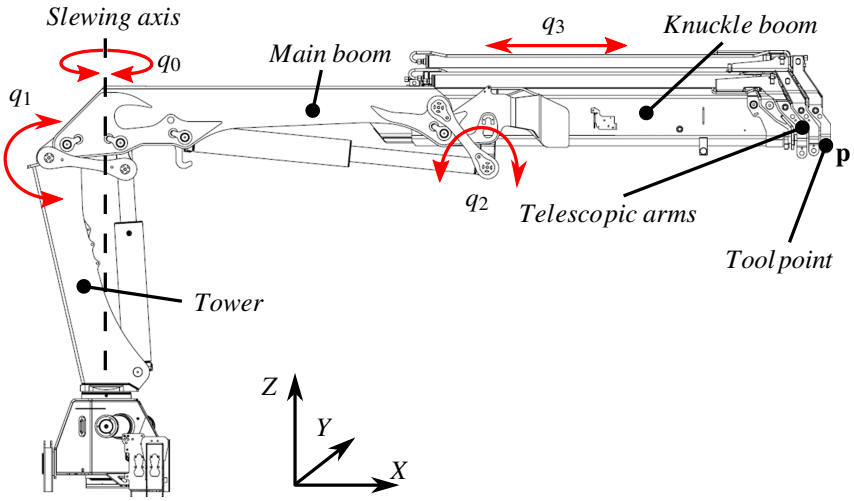

Figure 3.1: *Hydraulic actuated vehicle loader crane.*

The forward kinematics are relatively easy to set up, especially when employing

a systematic approach utilizing transformation matrices of the individual bodies of the crane. The main advantages of the forward kinematics are that, normally, the solution is unique and the demand for iterative solution of algebraic loops can be avoided. This is true as long as the crane has a kinematic structure with no or very simple closed loops.

3.1.3 Inverse Kinematics

The inverse position kinematics will give the joint position **q**, based on a tool point position **p**. It is however more complex to find the inverse kinematics of a serial manipulator such as a crane. As compared to the forward kinematics there are some challenges: it is possible to prescribe a none-feasible tool point position, it is very often the case that there are at least two possible sets of **q** that yield the same **p**, i.e., the solution to the inverse kinematics is not unique. An example of non-uniqueness is shown in Figure 3.2.

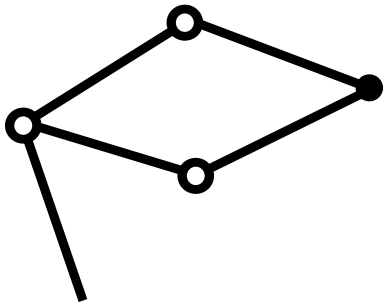

Figure 3.2: *Non-uniqueness, elbow up or elbow down.*

If the degrees of freedoms (DOFs) for the crane, which is the size of vector **q**, is bigger than the DOF of the tool point, size of **p**, $(n > m)$, then the manipulator has a redundant configuration. This means that it can have an infinite number of joint configurations for only one tool point position as seen in Fig. 3.3.

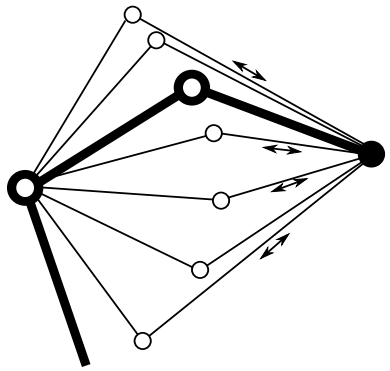

Figure 3.3: *Infinite joint configurations with a telescopic link.*

3.1.4 Velocity Kinematics

In addition to finding the tool point position, given a set of joint positions, the Cartesian tool point velocity based on the joint velocities can also be found using the Jacobian matrix.

$$\dot{\mathbf{p}} = \mathbf{J}(\mathbf{q})\dot{\mathbf{q}} \tag{3.2}$$

where $\dot{\mathbf{p}}$ is the tool point velocity which is normally prescribed in tracking and planned path operations. The vector $\dot{\mathbf{q}}$ contains the joint velocities.
$\mathbf{J}(\mathbf{q}) \in \mathbb{R}^{m\times n}$ is the Jacobian matrix, derived from the forward kinematics, defined as:

$$\mathbf{J} = \frac{\partial \mathbf{f}(\mathbf{q})}{\partial \mathbf{q}} \tag{3.3}$$

For a non-redundant crane, i.e. $(n = m)$ the required joint velocities can be found given a tool point velocity. This is done by inverting the Jacobian matrix and rearranging(3.2).

$$\dot{\mathbf{q}} = \mathbf{J}(\mathbf{q})^{-1}\dot{\mathbf{p}} \tag{3.4}$$

3.1.5 Redundant Manipulators

A redundant mechanism where the number of actuators exceeds the number of DOF of the tool point, leads to an infinite number of possible solutions to the inverse kinematics. Since $(n > m)$ the Jacobian matrix is no longer square, thus not invertible. This can, however, be resolved using the pseudo-inverse to solve the inverse kinematic problem.

$$\mathbf{J}^{\dagger} = \mathbf{J}^{T}(\mathbf{J}\mathbf{J}^{T})^{-1} \tag{3.5}$$

When using the pseudo-inverse Jacobian the general solution for the inverse kinematics is:

$$\dot{\mathbf{q}} = \mathbf{J}^{\dagger}\dot{\mathbf{p}} + (\mathbf{I} - \mathbf{J}^{\dagger}\mathbf{J})\dot{\mathbf{q}}_{\mathbf{0}} \tag{3.6}$$

Here $\mathbf{I} \in \mathbb{R}^{\mathbf{n}\times\mathbf{n}}$ is the identity matrix and $\dot{\mathbf{q}}_0 \in \mathbb{R}^{n}$ is an arbitrary joint velocity vector. The term $(\mathbf{I} - \mathbf{J}^{\dagger}\mathbf{J})$ defines the mapping into the null-space associated with $\mathbf{J}^{\dagger}$.

The Vector of the form $(\mathbf{I} - \mathbf{J}^{\dagger}\mathbf{J})\dot{\mathbf{q}}_{\mathbf{0}}$ produces only a joint self-motion of the structure, but no task space motion.

3.2 Dynamics

In mechanics, dynamics is the study of forces and torques and their effect on motion, as opposed to kinematics, which studies the motion of objects without reference to its causes. The dynamic model is important when designing a manipulator such as the crane, in simulation and in designing the control system algorithms. It can also be included in the algorithms itself, as model based control. By having a dynamic model of the manipulator, the torques and forces needed to move the manipulator can be calculated. This can be valued information in a control system algorithm. In the opposite way if a torque and force input are given to a manipulator, then resulting motion can be calculated from the dynamic model. This is used when a time domain simulation model is needed. Here the differential equations from the dynamic model are solved and the motion of the manipulator are calculated based

on the torque or force input. The dynamic model of a manipulator can be based on either a rigid body formulation or a flexible body formulation. In the latter case, the model complexity and simulation time invariably incresases. However, when introducing the dynamics and the flexibility of the mechanical system, it is also important to consider the dynamics and flexibility of the hydraulic system.

3.3 Hydraulic System

The manipulator and winch are hydraulically actuated. The vehicle loader crane has hydraulic cylinders to actuate each DOF and a hydraulic motor for the winch, see Figure 3.1. Each of the cylinders are operated by an electro-hydraulic directional control valve. The cylinder is also connected to a counter balance valve. The type of counter balance valve is different on each of the four cylinders, but the main functionality of the counter balance valve remains the same.

3.3.1 Modeling of a Hydraulic Pressure Compensated Flow Valve

Hydraulic valves are generally modeled as variable orifices with linear opening characteristics:

$$Q_v = C_v u \sqrt{\Delta p} \tag{3.7}$$

where u is the normalized opening of the valve, Δp is the differential pressure over the valve orifice and C_v is the valve coefficient:

$$C_v = C_d A_d \sqrt{\frac{2}{\rho}} \tag{3.8}$$

where C_d and A_d is the discharge coefficient and area, respectively. The oil density is denoted ρ.

The directional control valve can be models as four orifices, where the oil is directed to one of the two output ports of the valves. Similar, the oil is directed from the other output port to the return line, going to the oil reservoir. Some times it is necessary to improve the linearity of the valve in order to get good results, as done

in paper C.
In the pressure compensated DCV, the Δp term in (3.7) is held constant by a small compensator, as seen in Figure 3.4. With the term Δp constant, the flow Q_v is proportional to the opening u. As seen in the figure, the load pressure that is connected to the compensator is depending on which port A or B is active.

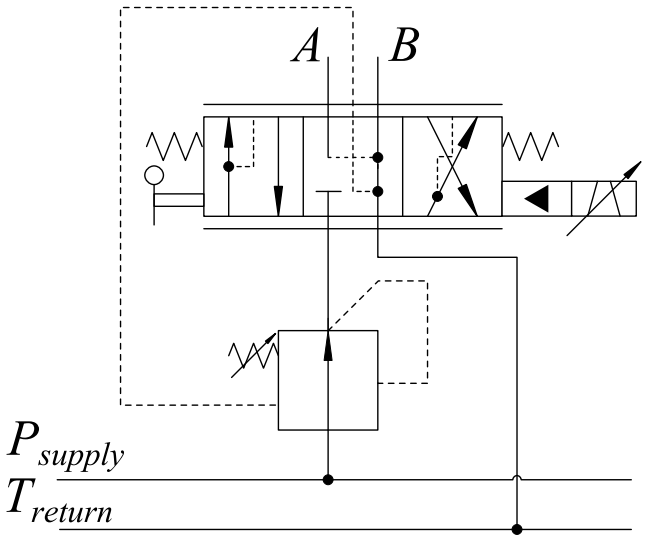

Figure 3.4: Pressure compensated directional control valve

The dynamics of the DCV can be described as a transfer function of a given order. In the literature, different order are used based on different situations. These valves are, normally, modeled as either a first or a second order system with a transfer function representing the spool travel vs. the valve control signal. A second order transfer function with the valves natural frequency ω_v and damping ζ_v, is given by:

$$G_{valve}(s) = \frac{1}{\frac{s^2}{\omega_v^2} + \frac{2\zeta_v s}{\omega_v} + 1} \tag{3.9}$$

$$Q_v(s) = Q_v^{ref}(s) \cdot G_{valve}(s) \tag{3.10}$$

where $Q_v(s)$ is the valve flow, and $Q_v^{ref}(s)$ is the reference flow given as a input signal to the valve.

The opening of the valve can be controlled by several different methods. It can be analogous by means of a voltage signal, or a current signal or it can be digitally using a data-bus, such as CAN bus which is used extensively in the mobile hydraulic industry.
Using the voltage signal V as the control signal, the valve is fully open when the signal is V_{max}, as shown in Figure 3.5. On the control spool in the valve there is a dead band that need to be exited in order for the valve to let the oil through. Otherwise the valve opening has a linear relation with the control signal.

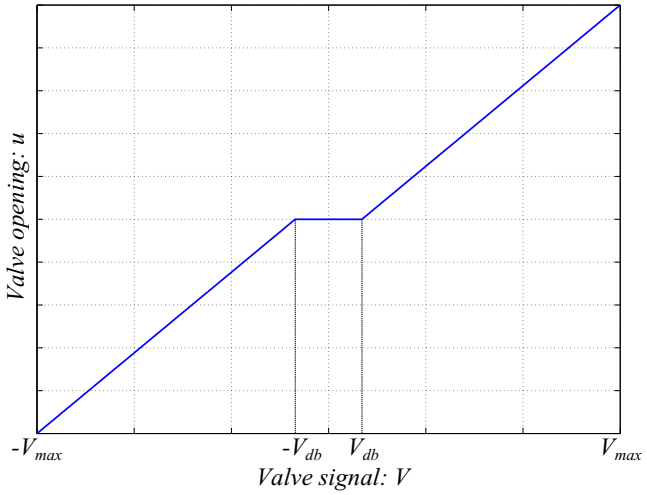

Figure 3.5: Valve Opening vs. Control Signal

To account for the dead band the control signal is based on the desired opening such as:

$$V = \left\{ \begin{array}{ccc} V_{db} + u \cdot (V_{max} - V_{db}) & , & u > 0 \\ 0 & , & u = 0 \\ -V_{db} + u \cdot (V_{max} - V_{db}) & , & u < 0 \end{array} \right\} \tag{3.11}$$

where V_{db} is the dead band voltage and V_{max} is the volt signal which corresponds to full valve opening.

3.3.2 Modeling of a Counter Balance Valve

Due to their tendency to cause oscillatory behavior, modeling and use of CBVs have been subject to quite extensive research. The model of the CBV consists of two components, both modeled according to (3.7). The components are a check valve and a pilot assisted relief valve as seen in Figure 3.6.

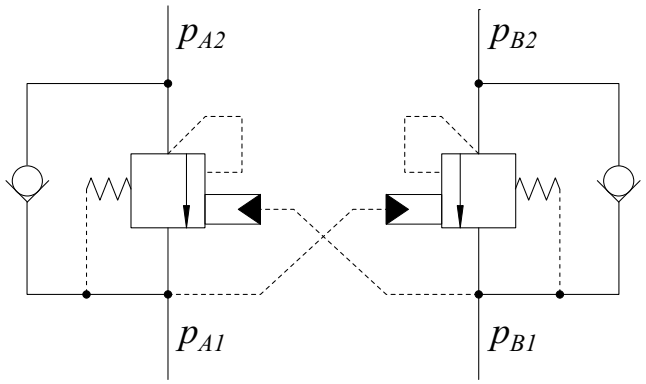

Figure 3.6: Double Counterbalance Valve

The dimensionless opening of the check valve (left in Figure 3.6) is:

$$u_{cv} = \frac{p_{A1} - p_{A2} - p_{cr,cv}}{\delta_{cv}} \tag{3.12}$$

where $p_{cr,cv}$ is the crack pressure of the check valve and δ_{cv} is the pressure equivalent spring rate.

For the CBV, the relative opening, also left in the figure, is:

$$u_{cbv} = \frac{p_{A2} + R \cdot p_{B1} - (R+1)p_{A1} - p_{cr,cbv}}{\delta_{cbv}} \tag{3.13}$$

where $P_{cr,cbv}$ is the crack pressure of the check valve, R is the pilot ratio of the port where P_{B1} is connected to and k_{cbv} is the pressure equivalent spring rate.

3.3.3 Modeling of Hydraulic Cylinder

Models of cylinders and their friction models have been topics for many researchers. Their complex friction forces, especially near zero velocity is described by different models, some more detailed then others. During the lifespan of the cylinder, the friction are bound to change due to the wear of the seals.

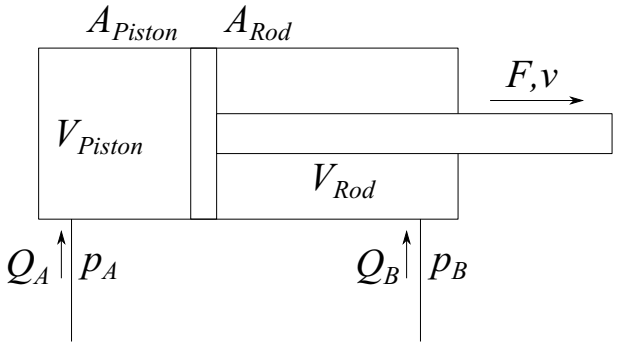

Figure 3.7: *Hydraulic Cylinder*

The force of a cylinder is determined by the area of active surfaces A_{Piston} and A_{Rod} in the cylinder and the pressure levels P_A and P_B, shown in Figure 3.7.
The force of the cylinder is describes as:

$$F = p_A \cdot A_{Piston} - p_B \cdot A_{Rod} - F_{friction} \cdot sign(v) \tag{3.14}$$

A_{Piston} is the surface area of the piston side of the cylinder, A_{Rod} is the area of the rod side, $F_{friction}$ is the friction force which is dependant of the direction the cylinder moves in and v is the velocity of the cylinder.
A simple model for friction is described by:

$$F_{friction} = F_S + C_p \cdot |F| \tag{3.15}$$

where F_S is the static friction force and C_p is the pressure dependant friction force.

The velocity of the cylinder is:

$$v = \frac{Q_A}{A_{Piston}} \tag{3.16}$$

The pressure gradient in the two chambers are a function of the flow going in and the change in volume of the chamber, and are described as:

$$\dot{P}_A = \frac{\beta}{V_A} \cdot (Q_A - v \cdot A_{Piston}) \tag{3.17}$$

$$\dot{P}_B = \frac{\beta}{V_B} \cdot (Q_B - v \cdot A_{Rod}) \tag{3.18}$$

where β is the bulk modulus of the oil.

3.4 Hoisting System

For the crane to pick up and place a payload on a moving vessel, a hydraulic winch can be used. Figure 3.8 shows the crane with the winch mounted on the telescopic knuckleboom. The winch enable the crane to reach a larger workspace.

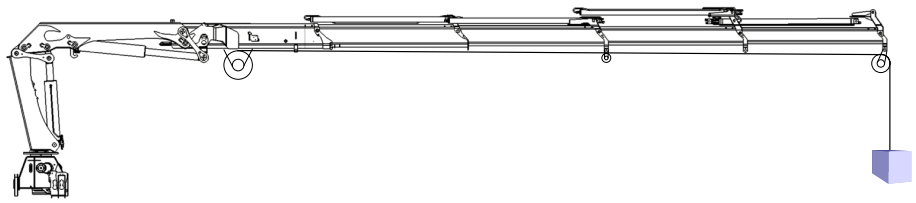

Figure 3.8: *Vehicle loader crane with attached winch system.*

The mechanical system consists of a hydraulic motor connected to a drum though a reduction gearbox. A steel wire is rolled on to the drum. The winch is mounted on a crane where the wire goes through a pulley, located at the tip of the crane. The mechanical system can be seen in Figure 3.9. In the figure B_m is the motor damping,

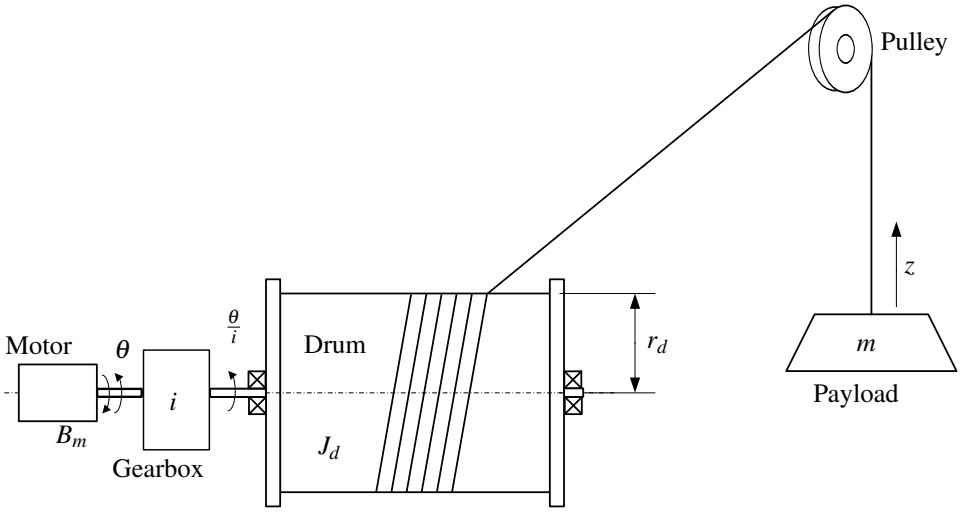

Figure 3.9: *Mechanical system*

i is the gear ratio of the gearbox, θ is the motor angle, J_d and r_d is the drum inertia and radius respectively, m is the payload mass and z is the vertical position of the payload.
The hydraulic system of the winch is shown in Figure 3.10:

The relation between motor angular velocity and the payload velocity is described:

$$\dot{z} = r_d \cdot \frac{1}{i} \cdot \dot{\theta} \tag{3.19}$$

The steady state flow equation for the valve is:

$$Q_v = C_v \cdot u \cdot \sqrt{\Delta P} \tag{3.20}$$

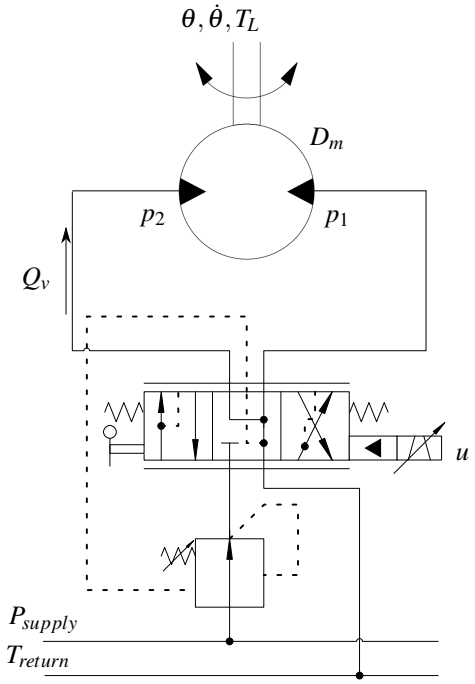

Figure 3.10: *Hydraulic system for winch*

where C_v is the valve constant, u is the normalized opening of the valve and ΔP is the differential pressure over the valve edge. By using a pressure compensated valve, a small hydraulic compensator is mounted before the control edge of the valve as seen in Figure 3.4. This compensator keeps the ΔP in the valve constant.
To analyse the hydro-mechanical system shown in Figure 3.9 and 3.10, the dynamic properties of the system is described mathematically. The valve dynamics is described by the first order transfer function:

$$G_v(s) = \frac{Q_v(s)}{u(s)} = \frac{K_v}{\tau s + 1} \tag{3.21}$$

where τ is the time constant for the valve and K_v is the valve gain:

$$K_v = C_v \cdot \sqrt{\Delta p} \tag{3.22}$$

The mass balance for the motor is:

$$\frac{V_f}{4\beta}\dot{p}_L = -K_{ce}p_L - D_m\dot{\theta} + Q_L \tag{3.23}$$

where V_f is the total volume of the fluids such as line, pipes and the motor, β is the effective bulk modulus of the system, $\dot{p}_L$ is the pressure gradient of the load pressure, K_{ce} is the leakage coefficient and D_m is the motor displacement.

The motor moment balance is described by

$$J_{eff}\ddot{\theta} = -B_m\dot{\theta} + D_m p_L - T_L \tag{3.24}$$

where B_m is the damping coefficient for the motor and load T_L is the load torque and J_{eff} is the effective moment of inertia seen from the motor:

$$J_{eff} = J_m + \frac{J_d}{i^2} + \frac{m \cdot r_d^2}{i^2} \tag{3.25}$$

where J_d and r_d is the drum inertia and radius respectively. J_m is the motor inertia, i is the gear ratio and m is the payload mass.
Taking the Laplace transformation of (3.23) and (3.24) results in the transfer function from the valve control signal to the velocity of the motor, assuming an infinitely fast valve

$$\dot{\theta} = \frac{\frac{K_v}{D_m}u - \frac{K_{ce}}{D_m^2}(1 + \frac{V_f}{4\beta K_{ce}}s)T_L}{\frac{s^2}{\omega_h^2} + \frac{2\zeta_h}{\omega_h}s + 1} \tag{3.26}$$

where ω_h is the hydraulic natural frequency:

$$\omega_h = \sqrt{\frac{4\beta D_m^2}{V_f J_{eff}}} \tag{3.27}$$

and ζ_h is the damping ratio:

$$\zeta_h = \frac{K_{ce}}{D_m}\sqrt{\frac{\beta J_{eff}}{V_f}} + \frac{B_m}{4D_m}\sqrt{\frac{V_f}{\beta J_{eff}}} \tag{3.28}$$

The transfer function (3.26) can be split up to the following two transfer functions

$$\frac{\dot{\theta}(s)}{u(s)} = \frac{\frac{K_v}{D_m}}{\frac{s^2}{\omega_h^2} + \frac{2\zeta_h s}{\omega_h^2} + 1} \tag{3.29}$$

$$\frac{\dot{\theta}(s)}{T_L(s)} = \frac{-\frac{K_{ce}}{D_m^2}(1 + \frac{V_f}{4\beta K_{ce}}s)}{\frac{s^2}{\omega_h^2} + \frac{2\zeta_h s}{\omega_h^2} + 1} \tag{3.30}$$

Eq. (3.29) assumes an infinitely fast valve response. In order to include the response of the valve, the following transfer function includes the contribution from (3.21)

$$G_{motor} = \frac{\dot{\theta}(s)}{u(s)} = \frac{\frac{\frac{K_v}{\tau s+1}}{D_m}}{\frac{s^2}{\omega_h^2} + \frac{2\zeta_h s}{\omega_h^2} + 1} \tag{3.31}$$

// Combining (3.19) and (3.32) describes the system from the valve signal to the velocity of the payload:

$$G_{system}(s) = \frac{\dot{z}(s)}{u(s)} = \frac{\frac{\frac{K_v}{\tau s+1}}{D_m}}{\frac{s^2}{\omega_h^2} + \frac{2\zeta_h s}{\omega_h^2} + 1}\frac{r_d}{i} \tag{3.32}$$

3.4.1 Identification

3.4.1.1 Hoisting System

To get a model that is similar to the real system a frequency response function (FRF) obtained by a open loop velocity feed-forward identification. A slow closed loop position feedback is implemented to keep the load from reaching any mechanical end stops.

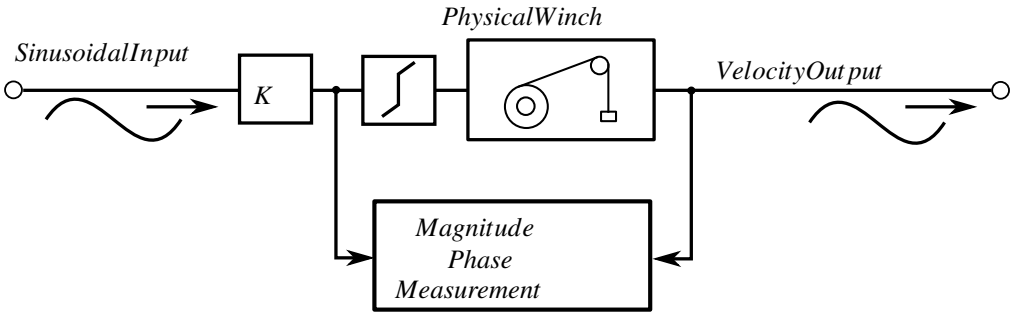

Figure 3.11: *Model Identification*

The input of the system is the valve opening signal and the output is the payload velocity, obtained by differentiating the measured position, which is based on a wire sensor connected between the crane tip and the payload.

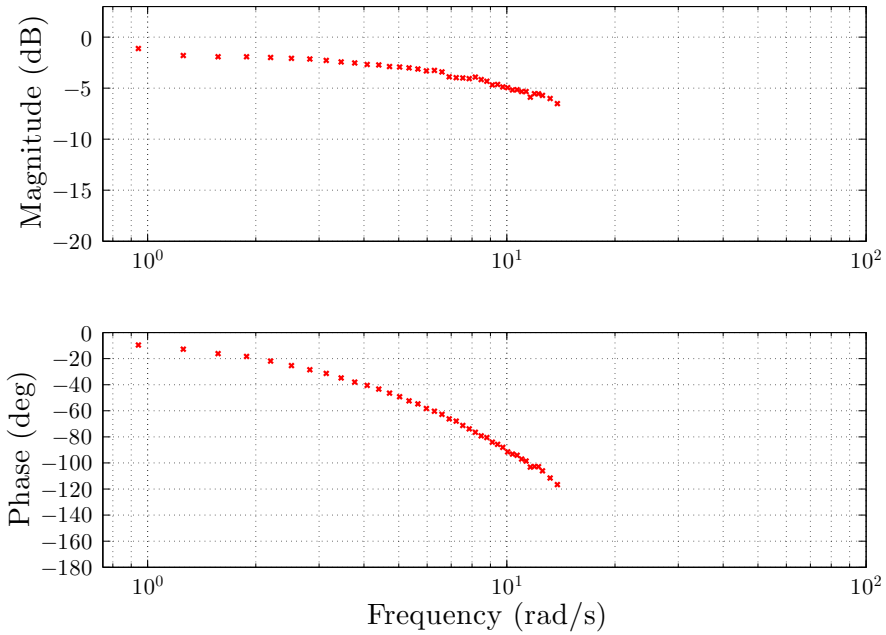

Figure 3.12: Measured Magnitude and Phase Shift for each Frequency

The excitation signal is a series of sinusoidal waves starting at $0.05Hz$ and $1.4Hz$. At each frequency the magnitude and phase shift is recorded. Figure 3.12 shows the measured magnitude and phase for each frequency.
The FRF is estimated as a transfer functions as shown in Figure 3.13.

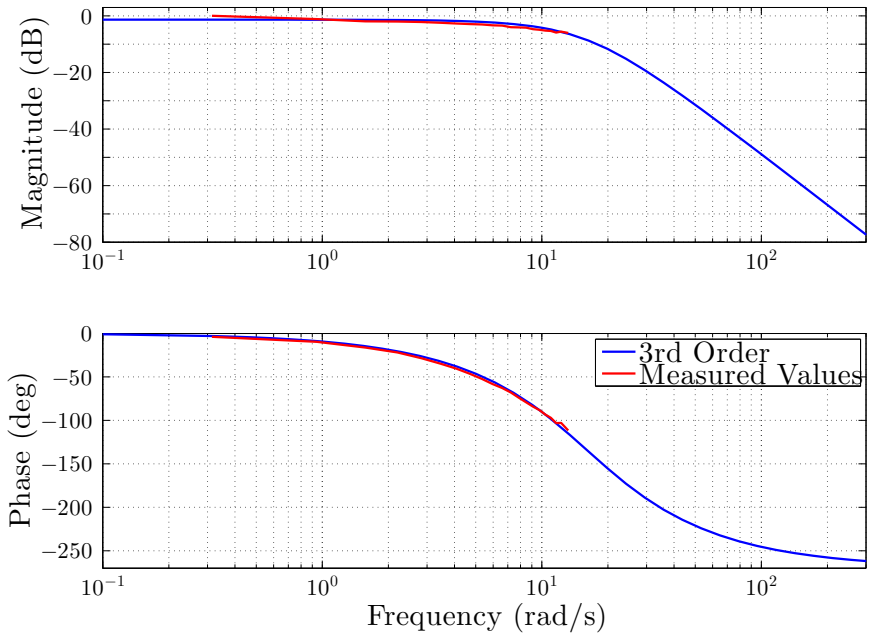

Figure 3.13: Estimation of Transfer Function for Valve and System Model: G_{system}

A good fit for the identification is the 3'rd order transfer function:

$$G_{system}^{est} = \frac{z_c}{p_3 s^3 + p_2 s^2 + p_1 s + p_c} \tag{3.33}$$

3.4.1.2 Slewing

The slewing mechanism from valve input to the en of the crane is modelled as a second order transfer function, see (3.34), with the system natural frequency and damping denoted as ωs and δs, respectively. Because the valve is pressure compensated, the speed vtp of the tool point is proportional to the input signal u, see (3.35).

$$G_s = K_s \frac{\omega_s^2}{s^2 + \delta\omega s + \omega_s^2} \tag{3.34}$$

$$v_{tp} = u \cdot G_s \tag{3.35}$$

The systems natural frequency and damping was found using a step input on the experimental crane. A transfer function was estimated to fit the response, shown in Figure 3.14. The experimental verified natural frequency and damping ratio is

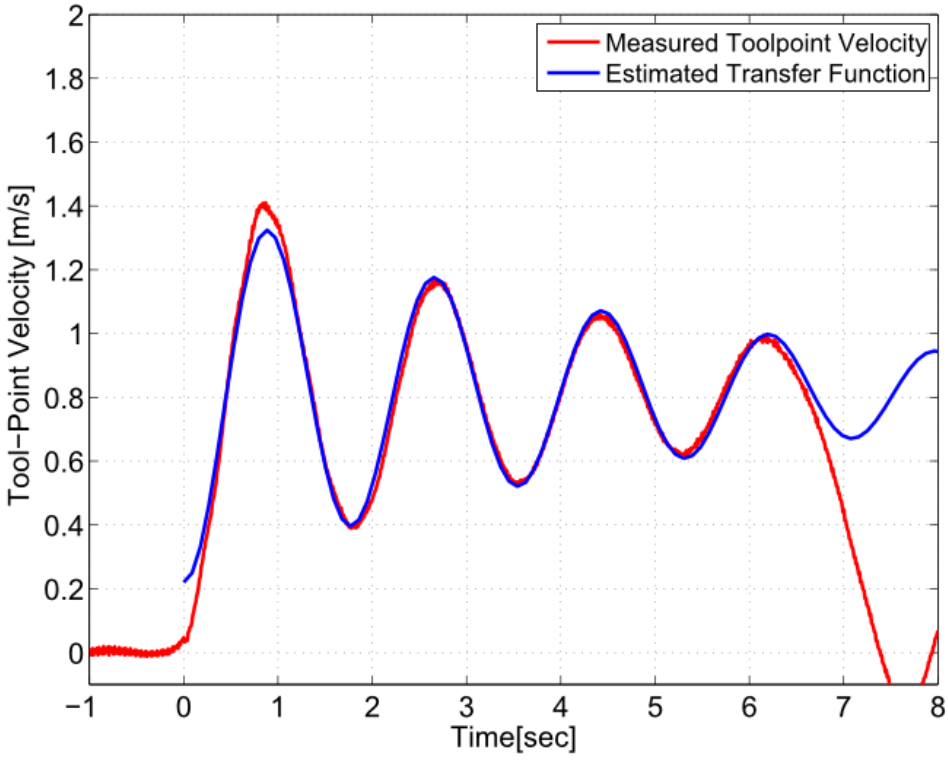

Figure 3.14: Estimation of transfer function for slewing

shown in 3.1.

Table 3.1: Damped natural frequency and damping ratio of crane.

Parameter		
ω_s	0.5	Hz
δ_s	0.1	-

Chapter 4

Control of Hydraulic Manipulators

Classically, motion control of hydraulic manipulators is the system that is designed to control one or more hydraulic valves so that the manipulator moves according to the desired reference. In general, there are two types of control of hydraulic manipulators. The first is by use of electro-hydraulic servo valves which have a very high dynamic response. These valves are often used in close loop systems where they provide high accuracy and stability when controlling position, velocity, and (less frequent) accelerations. These valves tend to have a high cost.
The other type of valve, which will be the focus of this thesis, is the proportional valve. This valve uses a mechanical spool to guide and control the amount of oil going through the valve. There are several types of proportional valves, but the focus will be on the pressure compensated directional control valve (DCV). In reference to the servo valves, the proportional valve tends to have a lower cost, but they have a slower response.

4.1 Manipulators

The rigid manipulator basically consist of bodies connected with joint, without any flexibility in joints or links. This is in reality never the case, as there will always be some flexibility in the foundation or by the deformation in the material that the bodies are made of. They are, however, much simpler to model than the flexible and

are therefore used much in computer simulations. Due to the lack of flexibility the manipulator will have a low mechanical resonance or high natural frequency.

4.1.1 Joint Control System

Joint control is the most basic and the inner control loop for the main purpose, tool point control. The tool point control mainly gives a set of joint reference to achieve the desired tool point, using the inverse kinematics. By knowing the joint position of the manipulator, the tool point can be calculated by the forward kinematics. Fig-

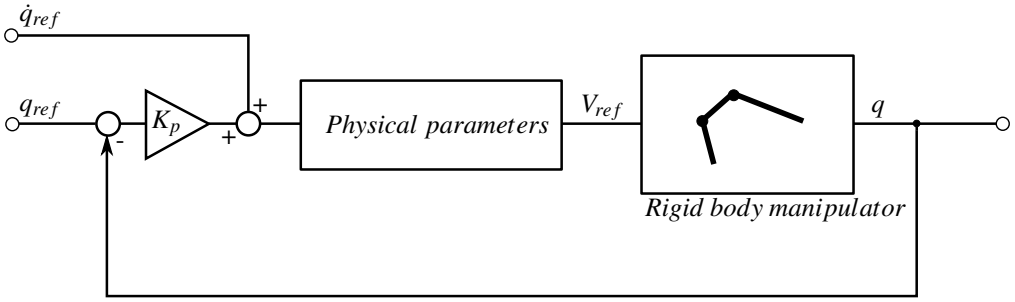

Figure 4.1: *Joint Control System for Rigid Manipulator*

ure 4.1 shows the control system for joint control of a rigid hydraulic manipulator. The block "Physical Parameters" contains the calculation such as geometric relations and parameters as valve and cylinders, shown in Figure 4.2. In Figure 4.2 the

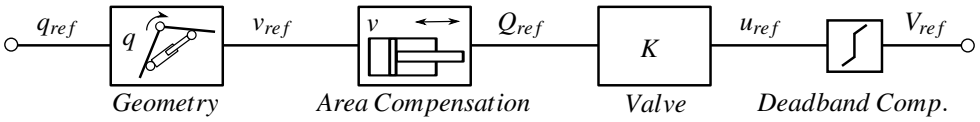

Figure 4.2: *Parameters*

blocks shown, includes "Geometry" which is the calculation of the linear cylinder motion from the angular joint motion. If the cylinder is mounted in parallel to a prismatic joint, the the transformation is 1. "Area Compensation" contains the flow needed to reach a velocity of a cylinder. Due to the fact that each of the cylinders has a different active area if the retract or extends, the function calculating the flow needed is dependant of the direction of the motion. The "Valve" block calculated

the valve opening needed to let through a correct amount of oil flow.
At last, the ”Deadband Comp.” block, adds an extra contribution to the signal to overcome the deadband of the valve.

4.2 Tool Point Control

Tool point control as opposed to joint control represents are more convenient and attractive way of using a manipulator. It focuses on the actual task of moving the tool point with its payload and, simultaneously, reduces the demands on skills and experience of the operator-in-the-loop. In automatic payload handling or heave compensation it's is almost a requirement. Description of the force relations and kinematics for control purpose of both the redundant and non-redundant manipulator, can be found in (Khatib and Burdick, 1986). For a non-redundant manipulator (NR), (n = m), the relations between the joint and tool point velocities are found using (3.4):

$$\dot{\mathbf{q}}_{NR} = \mathbf{J}^{-1}\dot{\mathbf{p}} \tag{4.1}$$

4.2.1 Redundant Manipulator

For a redundant manipulator, however, the jacobian matrix is non-square and not invertible, hence the pseudo-inverse of the Jacobian ($\mathbf{J}^{\dagger}$) is used as in (Whitney, 1969).

$$\mathbf{J}^{\dagger} = \mathbf{J}^{T}(\mathbf{J}\mathbf{J}^{T})^{-1} \tag{4.2}$$

Equation (4.2) defines the pseudo-inverse Jacobian which may replace J^{-1} in (4.1) yielding a new equation (4.3) which represents the relation between the joint and tool point velocities of the redundant manipulator.

$$\dot{\mathbf{q}} = \mathbf{J}^{\dagger}(\mathbf{q})\dot{\mathbf{p}} \tag{4.3}$$

Computing the joint velocities according to (4.3) corresponds to choosing the set of joint velocities that minimizes $\frac{1}{2}\dot{\mathbf{q}}^{T}\dot{\mathbf{q}}$ while meeting the tool point velocity con-

straint. In equation (4.4) the weighting matrix $\mathbf{W}$ is introduced so that the redundancy is handled by minimizing $\frac{1}{2}\dot{\mathbf{q}}^T\mathbf{W}\dot{\mathbf{q}}$. This makes it possible to take into account the velocity limits of each joint. The matrix $\mathbf{W} \in R^{n\times n}$ is a positive diagonal matrix and contains a weighting of each of the joint velocities.

$$\mathbf{W} = \begin{bmatrix} W_1 & 0 & 0 \\ 0 & W_2 & 0 \\ 0 & 0 & W_3 \end{bmatrix} \tag{4.4}$$

(4.5)

In this paper the following weighting is adopted:

$$W_i = \frac{1}{(v_i^U - v_i^L)^2}, \quad i = 1..3 \tag{4.6}$$

where v_i^U and v_i^L are the upper and lower limit, respectively, of the velocity of the i'th joint. A joint with a low velocity range will therefore be less activated during the operation. The following expression is obtained for the weighed pseudo-inverse Jacobian:

$$\mathbf{J}_W^\dagger = \mathbf{W}^{-1}\mathbf{J}^T(JW^{-1}J^T)^{-1} \tag{4.7}$$

A more general solution of (4.3) is presented by (4.8), where the weighted Pseudo-inverse Jacobian is used, see for example (Siciliano, 1990).

$$\dot{\mathbf{q}}_w = \mathbf{J}_\mathbf{W}^\dagger\dot{\mathbf{p}} + (\mathbf{I} - \mathbf{J}_\mathbf{W}^\dagger\mathbf{J})\dot{\mathbf{q}}_0 \tag{4.8}$$

Here $\mathbf{I} \in R^{n\times n}$ is the identity matrix and $\dot{\mathbf{q}}_0 \in R^n$ is an arbitrary joint velocity vector.

4.2.1.1 Nullspace

In (4.8) the null space mapping is introduced. The term $(\mathbf{I} - \mathbf{J}_w^{\dagger}\mathbf{J})\dot{\mathbf{q}}_0$ produces only a joint self-motion of the structure, but no task space motion. In other words, using the null-space motion allow the manipulator to change it pose without moving the tool point. This enables it to move into a more suitable pose, e.g. stiffer or more dexterous. It can also be used to make the manipulator to avoid the mechanical end limits in the structure.

A widely adopted approach is to solve the null space redundancy by optimizing the scalar cost function $h(\mathbf{q})$ using the gradient projection method, choosing $\dot{\mathbf{q}}_0$ to be the derivative of the cost function with regards to the joints, (4.9).

$$\dot{\mathbf{q}}_0 = \frac{\partial h}{\partial \mathbf{q}} \tag{4.9}$$

The cost functions (4.10) main goal is to avoid mechanical joint saturation, was introduced by (Ligeois, 1977) and used in (Pedersen et al., 2010) and (Chan and Dubey, 1993) before.

$$h(\mathbf{q}) = \frac{1}{3}\sum_{i=1}^{i=3}\left(\frac{\mathbf{q}_i - a_i}{a_i - y_i^U}\right)^n \tag{4.10}$$

$$a_i = \frac{y_i^U + y_i^L}{2} \tag{4.11}$$

$$n = [2,2,6] \tag{4.12}$$

where y_i^U and y_i^L are the upper and lower limit, respectively, of the joint i. Note that i starts from 1 and not from 0. This is due to that the slewing / joint q_0 has no redundancy. The mechanical joint end limits is shown in Table 4.1.

The slewing velocity reference is then given by: The tool point velocity is then

Table 4.1: Mechanical End Limits for Loader Crane

Joint	# Min Limit	# Max Limit	[-]
0	-180	180	degrees
1	-80	95	degrees
2	-120	5	degrees
3	0	10.5	meters

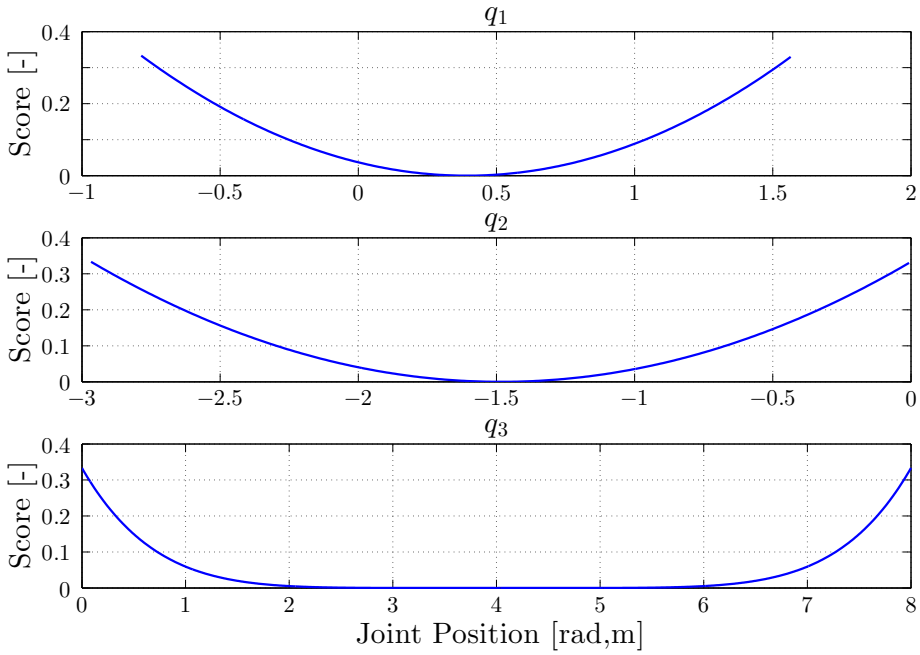

Figure 4.3: Nullspace Function

converted to joint velocities by:

$$\begin{bmatrix} \dot{q}_1 \\ \dot{q}_2 \\ \dot{q}_3 \end{bmatrix} = J_W^{\dagger} \begin{bmatrix} \dot{x} \\ \dot{z} \end{bmatrix} - (I - J_W^{\dagger} J)\dot{q}_{null} \tag{4.13}$$

The control equations is used in the control system for the crane is shown in Figure 4.5. Due to the difference of local and global coordinate system, and the transformation of task space to joint space, the control system includes some transformation blocks. The block ”Transform Task to Joint” uses (4.13). The block ”Physical

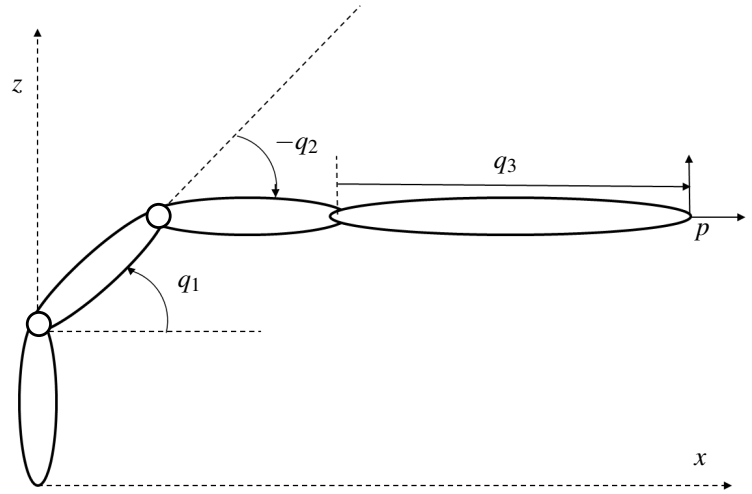

Figure 4.4: *Three DOF Manipulator - Planar*

Parameters" is described in Figure 4.2. The "Nullspace" block contains the last term in (4.8). Finally the block "Transform Joint to Task" is the forward kinematics, described by (3.1).

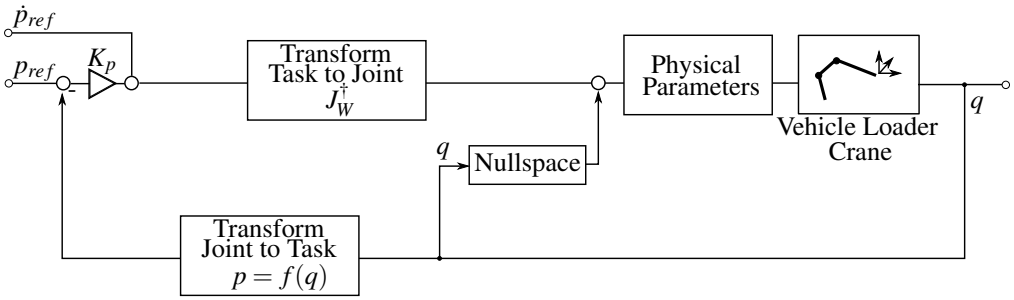

Figure 4.5: *Tool Point Control Circuit for Vehicle Loader Crane*

4.2.2 Pressure Feedback

An hydraulic system can be modeled based on (3.17) and (3.10), shown in Figure 4.6.

Implementing a lead compensation to the referenced flow results in inserting a first order filter based on the measured pressure, and is given by (4.14).

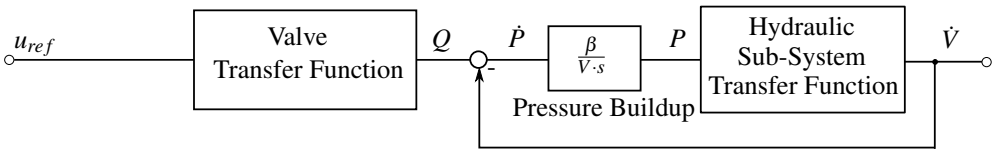

Figure 4.6: *Block Diagram for Simplified Circuit*

$$q_v^* = G_{Valve} \cdot (q_v^{ref} - K_f \frac{s \cdot p}{\frac{s}{\omega_f} + 1}) \tag{4.14}$$

The filter has two tunable parameters. The filter gain K_f and the filter frequency ω_f. Implementing the filter in the block diagram shown in Figure 4.6, results in a new block diagram with the filter as a feedback from the system pressure, which is easily available in the physical crane. Figure 4.7 shows the new block diagram including the feedback filter.

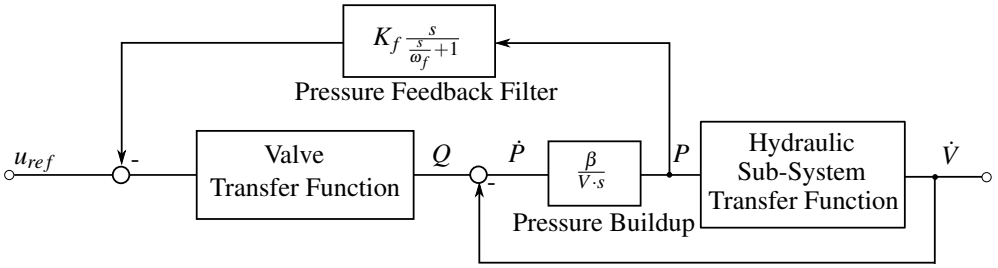

Figure 4.7: *Block Diagram for Simplified Circuit with Pressure Feedback*

Figure 4.8 shows an open loop bode plot is made for both the block diagram in Figure 4.6 and 4.7. It can be observed in the plot that the pressure feedback filter introduce an improved stability/phase margin. None of the systems are unstable, but when including the pressure feedback filter, the performance is improved.

4.2.3 Input Shaping

When a step/bang-bang command input is driven on a flexible system where two or more masses are connected in series with springs, the input will act on the first mass. This will cause a defection on the first spring, and will cause a series-reaction which

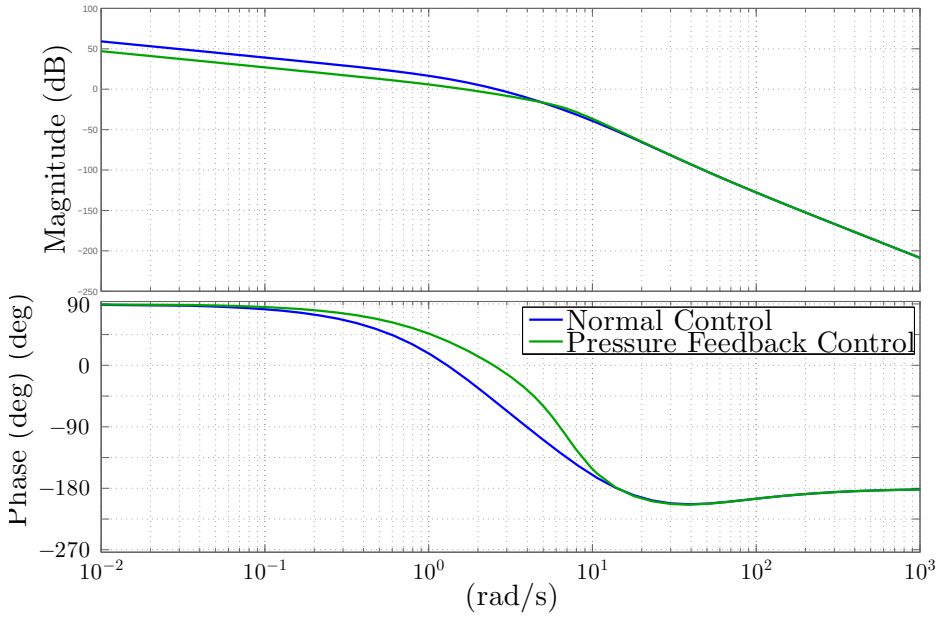

Figure 4.8: Bode Plot of Open Loop Transfer Function

will cause the whole system to start moving. Because the system is connected with springs, the whole system will start to oscillate. One way to reduce the oscillation is a have a slow ramp of the command signal, but this will introduce some negative effect as well, due to slower response.

By knowing just some information of the flexible system, it is possible to shape the shape the step/bang-bang commands so the it will drives the system without or with damped oscillation. By doing so, the system can be actuated fast and with reduced vibrations. It's however a little more complex than a slowly ramped signal because the information about the natural frequency and damping of the system should be known.

An example of a shaped signal is shown in Figure 4.9. In this figure, two positive impulses are creating a movement in a system. The first at $t = 1s$ and the second at $t = 1.5s$. Since the second impulse is given at the correct time and with a correct amplitude the system goes to rest.

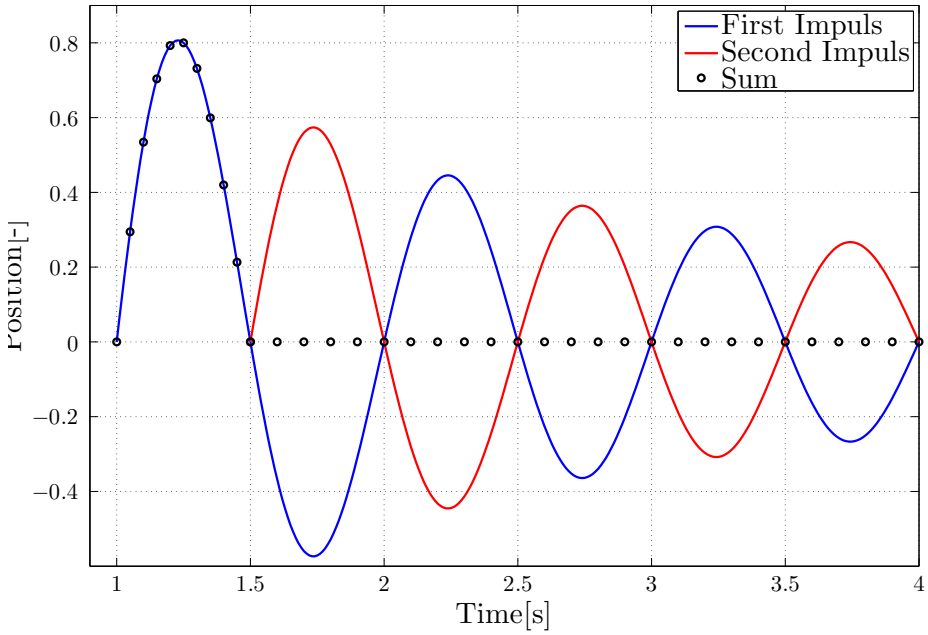

Figure 4.9: Example of Two Impulses Canceling Vibrations

The timing and amplitude as shown in the figure, can be found from the mathematical formulation of residual vibration from a sequence of impulses (4.15).

$$V(\omega_n, \zeta) = \mathrm{e}^{-\zeta \omega_n t_n} \sqrt{|C(\omega_n, \zeta|^2 + |S(\omega_n, \zeta|^2} \tag{4.15}$$

where

$$C(\omega_n, \zeta) = \sum_{i=1}^{n} A_i \mathrm{e}^{\zeta \omega_n t_i} \cos(\omega_d t_i) \tag{4.16}$$

and

$$S(\omega_n, \zeta) = \sum_{i=1}^{n} A_i \mathrm{e}^{\zeta \omega_n t_i} \sin(\omega_d t_i) \tag{4.17}$$

In (4.15) - (4.17), A_i is the amplitude and t_i is the time location of the impulses. n is the number of impulses in the impulse sequence. t_n is the time location of the final

impulse . ω_d is the damped natural frequency and is gives as:

$$\omega_d = \omega_n \sqrt{1-\zeta^2} \tag{4.18}$$

To obtain a normalized results and avoid zero valued impulses:

$$\sum_{i=1}^{n} A_i = 1 \tag{4.19}$$

The amplitude A_i could have both positive and negative values, but in this paper only the positive amplitude is considered. This is described by:

$$A_i > 0, i = 1...n \tag{4.20}$$

The goal for using the input shaping is to have zero residual vibration and to do this in the shortest time possible. The number of impulses is limited to 2, $n = 2$. To get zero residual vibrations, (4.15) must be equal to zero. This can only be done if both (4.16) and (4.17) is equal to zero independently. For simplicity $t_0 = 0$. Equations (4.19) and (4.20) also needs to be valid.
Substituting $t_1 = 0$ into (4.16) and (4.17) results in the following two equations:

$$0 = A_1 + A_2 e^{\zeta \omega_n t_2} \cos(\omega_d t_2) \tag{4.21}$$

$$0 = A_2 e^{\zeta \omega_n t_2} \sin(\omega_d t_2) \tag{4.22}$$

Solving for t_2 in the shortest time gives:

$$t_2 = \frac{\pi}{\omega_d} \tag{4.23}$$

The amplitudes A_1 and A_2 is based in the decay in the signal due to damping. If the case of an undamped system then $A_1 = A_2$. Given by (4.19) and thereafter

substituting for t_2 and (4.22):

$$A_1 + A_2 = 1 \tag{4.24}$$

$$0 = A_1 - (1 - A_1)\mathrm{e}^{\frac{\zeta\pi}{\sqrt{1-\zeta^2}}} \tag{4.25}$$

Using the experimentally verified data and inserting them into (4.24) and (4.25) gives the solution for the two amplitudes and timing of the second impulse. This is the main focus in Paper D.

4.3 Hoisting System

4.3.1 Heave Compensation

To perform heave compensation, a motion sensor is used which enables measurement of the acceleration, velocity and position of the moving target. The goal for the winch system is to track this motion. The controller shown in Figure 4.10 is used for this purpose and is a position feedback + velocity feed forward controller. Based on system identification, the system to control is the transfer function described by eq.(3.33).

$$C = P_p(P_{ref} - z) + P_v V_{ref} + P_a A_{ref} \tag{4.26}$$

Where K_p, K_v and K_a are proportional gains for position, velocity and acceleration respectively.

There is a dead-band compensator to avoid the dead-band in the spool of the hydraulic valve, given by eq.(3.11). P_{ref}, V_{ref} and A_{ref} are the reference position, velocity and acceleration that are measured by a sensor.

The Bode plot in Figure 4.11 shows the open and the closed loop response of the system in eq.(3.33), using the proposed controller shown in Figure 4.10.

The closed loop system gives a good tracking over the frequencies. Normal wave periods can be from 4 to 16 s. At 4s the closed loop Bode plot shows a

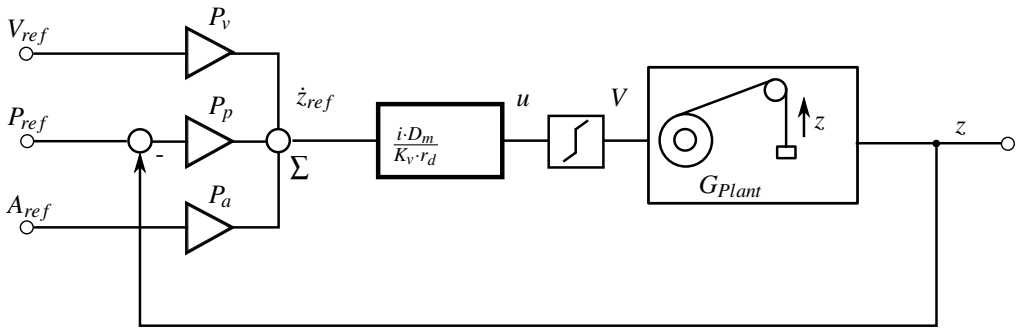

Figure 4.10: *Control Circuit Strategy*

magnitude of 0.0896 dB and the phase lag is $-9.94°$.

4.3.2 Constant Tension

By turning the position of the hydraulic motor, the wire is stretched. Based on the flexibility of the crane, it is possible to control the winch tension, thus the tension in the load. A closed feedback loop P controller is used to control the velocity of the motor as shown in Figure 4.12.

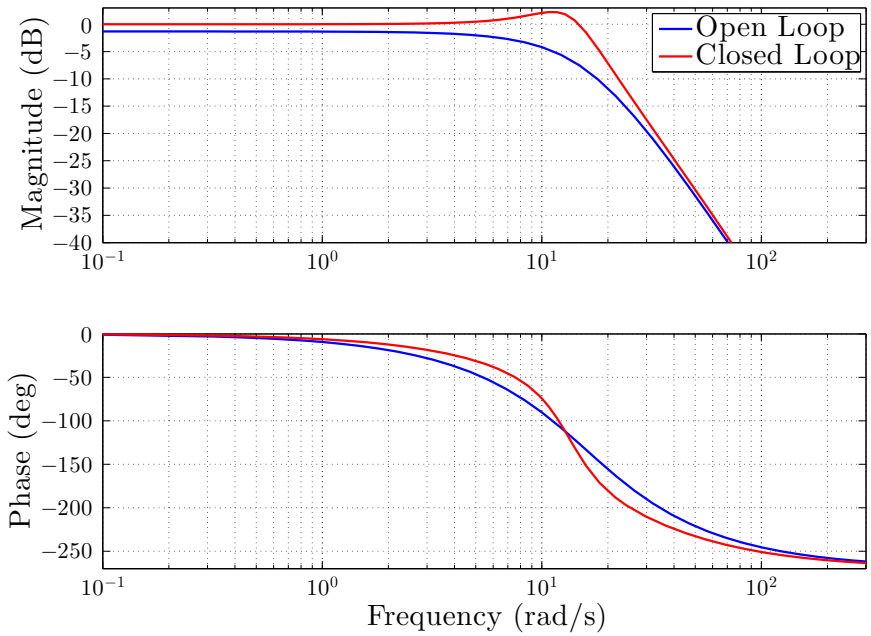

Figure 4.11: Closed loop Bode plot

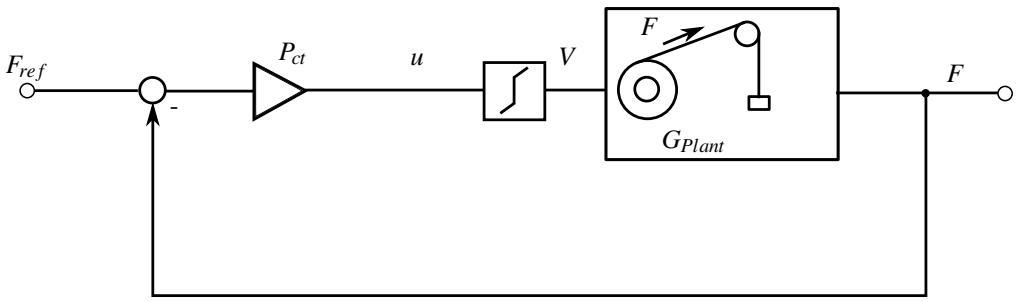

Figure 4.12: *Control Circuit for Constant Tension*

Chapter 5

Concluding Remarks

5.1 Conclusions

The work shown in this thesis focus on the use of knuckle boom cranes as hydraulically actuated manipulators for payload transfer in an offshore environment characterized by wave induced motion disturbances. This calls for motion compensated tool point control and a number of issues have been investigated under this topic. The PhD project has not focused on the laws and safety regulations for offshore load transferring, neither does it concern itself directly with durability and environment protection for such a crane. The focus has been on the modeling and control, where the control is specialized in what is needed in a marine operation, such as the offshore payload transfer to and from a floating vessel.

There has been great focus on doing physical experiments and there has been put much effort into getting the theory into practice and implementing the control strategies into physical machinery. Firstly, redundancy has been investigated since the knuckle boom cranes are typical hydraulically actuated manipulators that encompass several degrees of freedom: swing, main boom, knuckle boom, telescope and winch, however, with a free hanging payload there is also non-actuated degrees of freedom. In this project work on redundancy was mainly carried out on a planar 3-DOF manipulator with payload capacity of less than 100 kg and actuated by means of three servo valves. The redundancy was solved using the pseudo-inverse Jacobian method exploiting null space joint motion to handle joint saturation and

actuator velocity minimization. Tool point velocity control of the manipulator was obtained with a model based feed-forward controller, combined with a PI feedback controller. When adding a free hanging payload the compensation of the un-actuated degree of freedom employed LQR control, minimizing position and velocity error while maintaining the tracking reference for the tool point. All of the developed methods where investigated numerically by means of simulation models but also implemented on the actual machine mounted on a Stewart platform. This allowed for the introduction of wave disturbances in a dry environment and an experimental verification. For both systems the proposed control schemes worked satisfactory and it seems feasible to see this implemented on larger cranes with a suitable instrumentation including feedback from any un-actuated degree of freedom of the free hanging payload.

The use of servo valves on the 3-DOF manipulator disguises a common problem when working with hydraulically actuated manipulators namely the oscillatory nature obtained by combining directional control valves using pressure compensated metering-in flow with counterbalance valves while handling negative loads. This issue was addressed by investigating the use of a pressure gradient feedback scheme that was introduced to both a 1-DOF manipulator with a load capacity of 500 kg and a commercial 4-DOF vehicle loader crane with a load capacity of 150 kNm (1200 kg @ 12 m). In both case a relatively simple pressure feedback scheme aiming at removing any oscillations in the inlet pressure by superimposed on the nominal valve control signal effectively removed or minimized an otherwise predominant oscillatory nature of the hydraulic-mechanical system.

Using the commercial 4-DOF vehicle loader crane the pressure feedback approach was combined with a novel way of handling the flexibility of the crane. Emphasis was put on the slewing motion and the input shaping method that has been developed for hanging payloads was introduced. Input shaping is basically a feed forward control and the underlying idea for introducing it is that the dominant low eigenfrequency of a commercial vehicle loader crane, in this case the one associated with the slewing motion, is so low that it can be handled as a free hanging load. This gave some very encouraging results when tested numerically and experimentally and it was clear that the tool point control benefited heavily from the combination of pres-

sure feedback and input shaping with pressure feedback handling oscillations associated with small velocities and hydraulic-mechanical instability and input shaping handling oscillations associated with start and stop especially at higher velocities. This was also confirmed with the two methods implemented separately. This very promising combination could, if time had allowed, been combined with the LQR method introduced for free hanging loads on the 3-DOF manipulator but time did not allow for that.
The use of the commercial 4-DOF vehicle loader crane introduces both difficulties and possibilities in tool point motion control due to its low mechanical flexibility and, subsequent, low dominant eigenfrequencies. Offshore cranes are, however, not used for motion only but also very much for constant tension applications. In that case a winch suspended wire hanging from the tool point must be held at a constant tension. In that case the flexibility of the crane can be utilized. A novel control strategy including heave compensation and constant tension modes using both feedforward from a motion reference unit as well as feedback from a load cell introduced exploiting the flexibility of the crane structure. For that purpose the 4-DOF vehicle loader crane had a 5th DOF added in the shape of a hydraulically actuated winch. The experimental results where very encouraging and this is an important aspect of the potential exploitation of the flexibility of commercial knuckle boom cranes that is closely related to the successful introduction of input shaping mentioned earlier. In general, a number of important issues related to the use of knuckle boom cranes for offshore payload transfer between vessels have been investigated and the overall contribution of this work is that it has been shown that it is feasible to use commercial available knuckle boom cranes for offshore heave compensation both on tool point motion control, hanging payload control and winch suspended wire tension control.

5.2 Contribution to Knowledge

Paper A:
Paper A deals with the tool point control for compensation keeps the loading point fixed in reference to the target platform. The scaled hydraulic manipulator con-

trolled by servo valves were controlled by a feed forward control signal with a closed loop position feedback. Experimental verification include placing the manipulator on a moving platform, simulation a floating vessel.

Paper B:

Paper B deals with the stabilization of a hanging load. The load is connected to the tool point of the manipulator. The stabilization algorithm, based on a LQR control strategy, reduce vibration in the hanging load, while the manipulator moves its tool point from A to B. The experimental results shows that the vibration is reduced under this movement, but also when a disturbance is caused.

Paper C:

Paper C deals with an electronic pressure compensation control scheme is put forward that allows the use of non-compensated directional control valves in closed loop motion control. The control scheme measure the pressure drop across the metering-out orifice and continuously adjusts a feed forward gain that is computed based on a preprocessing of the valve characteristics. The experimental conducted in this paper the proposed scheme gives a better performance than a pressure compensated circuit (difference in oscillation level) and a better performance than a non-compensated circuit with constant feed forward (less sensitive to load variations). In general, the proposed scheme seems to be a realistic alternative within motion control of hydraulic actuators.

Paper D:

Paper D deals with the development of an active vibration damping control for the slewing motion of a hydraulic vehicle loader crane. The control strategy combines the input shaping filtration with the pressure feedback and together they are damping the vibrations caused from the hydraulic and the mechanical elements of the crane. It can be seen in the experimental results that the pressure feedback has the most effect on the low velocity and less effect on the higher. For the input shaping it is opposite, low effect at low velocity and most effect on high. For the pressure feedback this can be explained by the effects of the counterbalance valves since they tend to be more stable at higher velocities when the pressures in the systems are higher. The results shows a significant reduction in crane vibrations on all three velocity references.

Paper E:
Paper E deals with the hoisting system on the crane. An experimental frequency response of the hydraulic winch is made. Using this model, the control system is developed for actively heave compensating the payload while landing it on the moving platform. The payload is lifted by having a constant wire tension. Using the flexibility of the vehicle loader crane, the wire tension is controlled by turning the winch. Experimental work includes lifting and landing on a moving Stewart platform.

5.3 Future Work

As the trend in the offshore wind community heads to move the wind turbines into deeper water, the need for access solution for floating wind turbines are required. By placing a manipulator such as the mobile crane on top of a Stewart platform and performing a payload transfer onto another Stewart platform would give a useful knowledge on vessel to vessel payload transfer.

REFERENCES

(2013). NSLT - The 18^{th} North Sea Offshore Crane and Lifting Conference, Stavanger, Norway - Norwegian Society of Lifting Technology.

Ampelmann (2015). Offshore Access System. `http://www.ampelmann.nl/`. [Online; accessed 09-June-2015].

Bakka, T. (2013). *Multiobjective optimization and multivariable control of offshore wind turbine system*. PhD thesis, University of Agder.

Beiner, L. and Mattila (1999). An improved pseudoinverse solution for redundant hydraulic manipulators. *Robotica*, 17:173–179.

Chan, T. F. and Dubey (1993). Weighted least-norm solution based scheme for avoiding joint limits for redundant manipulators. *Robotics and Automation*, 3:395–402.

Chapple, P. J. and Tilley, D. G. (1994). Evaluation techniques for the selection of counterbalance valves. In *Proc. of The Expo and Technical Conference for Electrohydraulic and Electropneumatic Motion Control Technology, Anaheim, USA*.

Chunhacha, P. and Benjanarasuth, T. (2011). Parameters tuning effects in the model predictive control of an inverted pendulum. In *TENCON 2011 - 2011 IEEE Region 10 Conference*, pages 1080–1084.

Cinkelj, J., Kamnik, R., Cepon, P., Mihelj, M., and Munih, M. (2010). Robotic control system for hydraulic telescopic handler. In *Robotics in Alpe-Adria-Danube Region (RAAD), 2010 IEEE 19th International Workshop on*, pages 137 –142.

Ebbesen, M., Hansen, M., and Andersen, T. (2006). Optimal tool point control of hydraulically actuated flexible multibody system with an operator-in-the-loop. In *In III European Conference on Computational Mechanics*, pages 568–568, Springer Netherlands.

Engedal, H. and Egelid, P. M. (2011). Modeling, simulation, and testing of constant tension system on winch. diploma thesis, University of Agder.

Entao, Z. and Wenlin, Y. (2009). Research on the motion tracking feedforward control of hydraulic winch. In *Computer Engineering and Application, 2009 International Conference on*.

Entao, Z., Wenlin, Y., and Junzhe, L. (2009). Predictive control of hydraulic winch motion control. In *Computer Science and Information Technology, 2009. ICCSIT 2009. 2nd IEEE International Conference on*, pages 1–4.

EWEA (2013). Deep water the next step for offshore wind energy. Technical report, European Wind Energy Association.

H Handroos, J. H. and Vilenius, M. (1993). Steady state and dynamic properties of counterbalance valves. In *Proc. of 3rd Scandinavian International Conference on Fluid Power, Linkping, Sweden*.

Haaø, J., Vangen, S., Tyapin, I., Choux, M., Hovland, G., and Hansen, M. R. (2012). The effect of friction in passive and active heave compensation of crown block mounted compensators. In *2012 IFAC Workshop on Automatic Control in Offshore Oil and Gas Production*.

Han, J. and Chung, W. K. (2007). Redundancy resolution for underwater vehicle-manipulator systems with minimizing restoring moments. In *Intelligent Robots and Systems, 2007. IROS 2007. IEEE/RSJ International Conference on*, pages 3522 –3527.

Hansen, M. R. and Andersen, T. O. (2010). Controlling a negative loaded hydraulic cylinder using pressure feedback. In *Proc. of IASTED International Conference Modelling, Identification, and Control : Proceedings Innsbruck, Austria*.

Imanishi, E., Nanjo, T., and Kobayashi, T. (2009). Dynamic simulation of wire rope with contact. *Journal of Mechanical Science and Technology*, 23(4):1083–1088.

Johansen, T., Fossen, T., Sagatun, S. I., and Nielsen, F. (2003). Wave synchronizing crane control during water entry in offshore moonpool operations - experimental results. *Oceanic Engineering, IEEE Journal of*, 28(4):720–728.

Khatib, O. and Burdick, J. (1986). Motion and force control of robot manipulators. In *Robotics and Automation. Proceedings. 1986 IEEE International Conference on*, volume 3, pages 1381–1386.

Kucuk, S. and Bingul, Z. (2004). The inverse kinematics solutions of industrial robot manipulators. In *Mechatronics, 2004. ICM '04. Proceedings of the IEEE International Conference on*, pages 274 – 279.

Ligeois, A. (1977). Automatic supervisory control of the configuration and behavior of multibody mechanisms. *IEEE Trans. Systems Man Cybernet*, 7:868–871.

Miyakawa, S. (1978). Stability of a hydraulic circuit with a counterbalance-valve. In *Bulletin of the JSME*.

Moon, K. (2012). Input shaping control for suppression of boom vibrations. In *Automation Science and Engineering (CASE), 2012 IEEE International Conference on*, pages 782–785.

Neupert, J., Mahl, T., Haessig, B., Sawodny, O., and Schneider, K. (2008). A heave compensation approach for offshore cranes. In *American Control Conference, 2008*, pages 538–543.

Nordhammer, P., Bak, M., and Hansen, M. (2012). Controlling the slewing motion of hydraulically actuated cranes using sequential activation of counterbalance valves. In *Control, Automation and Systems (ICCAS), 2012 12th International Conference on*, pages 773–778.

Overdiek, G. (1980). Dynamisches verhalten von senkbrems- sperrventilen im hydraulik-hubwerk. In *lhydraulik und Pneumatik*.

Overdiek, G. (1981). Design and characteristics of hydraulic winch controls by counterbalance valves. In *European Conference on Hydrostatic Transmissions for Vehicle Applications, Aachen*.

P A Nordhammer, M. K. B. and Hansen, M. R. (2012). A method for reliable motion control of pressure compensated hydraulic actuation with counterbalance valves. In *Proc. of 2012 ICCAS12 12th International Conference on Control, Automation, and Systems, Jeju, Korea*.

Palfinger (2015). Wind Cranes. `https://www.palfinger.com/en/marine/products/wind-cranes`. [Online; accessed 09-June-2015].

Park, J., Choi, Y., Chung, W. K., and Youm, Y. (2001). Multiple tasks kinematics using weighted pseudo-inverse for kinematically redundant manipulators. In *Robotics and Automation, 2001. Proceedings 2001 ICRA. IEEE International Conference on*, volume 4, pages 4041 – 4047 vol.4.

Pedersen, M. M., Hansen, M. R., and Ballebye, M. (2010). Developing a Tool Point Control Scheme for a Hydraulic Crane Using Interactive Real-time Dynamic Simulation. *Modeling, Identification and Control*, 31(4):133–143.

Perez, T. (2005). Course keeping and roll reduction using rudder and fins, advances in industrial control. In *Ship motion control:*. London: Springer.

Power, O. (2015). Maxcess. `http://www.osbitpower.com./technology/maxccess`. [Online; accessed 09-June-2015].

Siciliano, B. (1990). Kinematic control of redundant robot manipulators: A tutorial. *Journal of lntelligent and Robotic Systems*, 3:201–212.

Siciliano, B., Sciavicco, L., Villani, L., and Oriolo, G. (2010). *Robotics- Modelling, Planning and Control*. Springer.

Singhose, W. and Seering, W. (2011). *Command Generation for Dynamic Systems*. Lulu.

Sorensen, K., Hekman, K., and Singhose, W. (2010). Finite-state input shaping. *Control Systems Technology, IEEE Transactions on*, 18(3):664–672.

Spong, M. W., Hutchinson, S., and Vidyasagar, M. (2006). *Robot Modeling and Control*. Wiley.

Sverdrup-Thygeson, J. (2007). Modeling and simulation of an active hydraulic heave compensation system for offshore cranes. diploma thesis, Norwegian University of Science and Technology.

T Persson, P. K. and Palmberg, J. O. (1989). Properties of over-center valves in mobile systems. In *Proc. of 2nd International Conference on Fluid Power Transmission and Control, Hangzhou, China*.

Than, T. K., Langen, I., and Birkeland, O. (2002). Modelling and simulation of offshore crane operations on a floating production vessel.

Uptime (2015). Gangway. `http://www.uptime.no/`. [Online; accessed 09-June-2015].

Wen, B., Homaifar, A., Bikdash, M., and Kimiaghalam, B. (1999). Modeling and optimal control design of shipboard crane. In *American Control Conference, 1999. Proceedings of the 1999*, volume 1, pages 593–597.

Whitney, D. E. (1969). Resolved motion rate control of manipulators and human prostheses. *IEEE Trans. Man-Machine Systems*, 10:47–53.

Yuan, Q. (2010). Actively damped heave compensation (adhc) system. In *American Control Conference (ACC), 2010*, pages 1544–1549.

appendix 1

==========

appendix 2

appendix 3

appendix 4

appendix 5